Editors

Assoc. Prof. Dr. Sadi ELASAN - Instructor Fırat KESKİN

STATISTICAL METHODS USED IN IMAGE PROCESSING AND AN APPLICATION

Dr. Yusuf DİLBİLİR
Prof. Dr. Sıddık KESKİN
Assoc. Prof. Dr. Musa ATAŞ

DUVAR

STATISTICAL METHODS USED IN IMAGE PROCESSING AND AN APPLICATION

Authors

Dr. Yusuf DİLBİLİR
Prof. Dr. Sıddık KESKİN
Assoc. Prof. Dr. Musa ATAŞ

Editors

Assoc. Prof. Dr. Sadi ELASAN
Instructor Fırat KESKİN

[1] This study was adapted from the Master's thesis of Dr. Yusuf DİLBİLİR, supervised by Prof. Dr. Sıddık KESKİN and Assoc. Prof. Dr. Musa ATAŞ. In addition, the application material of the study was provided by the projects numbered "113E620" and "2150154" supported by The Scientific and Technological Research Council of Türkiye (TÜBİTAK).

Statistical Methods used in Image Processing and an Application

Dr. Yusuf DİLBİLİR
Prof. Dr. Sıddık KESKİN
Assoc. Prof. Dr. Musa ATAŞ

Editor in chief: Berkan Balpetek
Editors: Assoc. Prof. Dr. Sadi ELASAN, Instructor Fırat KESKİN
Cover and Page Design: Duvar Design
Printing : December -2023
Publisher Certificate No: 49837
ISBN: 9978-625-6585-60-7

853 Sokak No:13 P.10 Kemeraltı-Konak/İzmir Tel: 0 232 484 88 68

www.duvaryayinlari.com
duvarkitabevi@gmail.com

ACKNOWLEDGEMENT

This study was adapted from the Master's thesis of Dr. Yusuf DİLBİLİR, supervised by Prof. Dr. Sıddık KESKİN and Assoc. Prof. Dr. Musa ATAŞ. In addition, the application material of the study was provided by the projects numbered "113E620" and "2150154" supported by The Scientific and Technological Research Council of Türkiye (TÜBİTAK).

We would like to thank Van Yüzüncü Yıl University, Institute of Health Sciences, Department of Biostatistics; Siirt University, Faculty of Engineering, Computer Engineering, Al-Jazari Cybernetics and Robotics Laboratory and TÜBİTAK for providing all kinds of contributions and support for the conduct of the study.

TABLE OF CONTENTS

SYMBOLS AND ABBREVIATIONS

a	: Constant number
AIC	: Akaike's Information Criteria
B	: Blue
b	: Coefficient of the independent variable
BIC	: Bayesian Information Criteria
DPI	: Dots Per Inch
F	: Frequency
G	: Green
A Weight	: Actual Weight
A WIDTH	: Actual Width
A LENGTH	: Actual Length
MSE	: Mean Squared Error
SSE	: Sum of Squared Error
k	. Number of independent variables in the regression model
EAR	: Edge-to-Area Ratio
r	: Number of rows
MCp	: Mallows' Cp statistic
c	: Number of columns
n	: Number of observations
nm	: Nanometer
OCL	: Open Cezeri Library
Dpi	: Dots Per Inch
Ppi	: Pixels Per Inch
R	: Red
R^2	: Coefficient of determination
$R^2_{(Adj)}$	: Adjusted determination coefficient
RGB	: Red, green blue color space
T	: Time
TEL	: Total Edge Length
X	: Independent variable
Y	: Dependent variable
Z	: Depth
Λ	: Color
σ^2	: Variance

LIST OF FIGURES

LIST OF TABLES

1. INTRODUCTION

With the successful developments in technology day by day, products that make human life significantly easier have been discovered. There is no doubt that computers have an important role in these developments. Artificial intelligence supported machines that make human life easier have been invented by using various software and hardware that connects these software to real life. Thus, the need for manpower in the works done has been minimized and the works have been carried out more quickly and safely. It is possible to recognize these benefits of technology in many areas such as education, defense, health, industry and science.

Acquiring symptoms such as sound, heat, light and movement through relevant sensors and converting these inputs into digital data is called signal processing. One of the most important and fast-developing areas of signal processing technology is image processing.

With image processing methods, properties of the image such as color, resolution, brightness and structure can be changed and solutions to various problems can be found with this data. These processes can be used to eliminate visual distortions caused by software or hardware, as well as in many areas such as detection, recognition and tracking of objects. Using image processing methods, features such as width, length, perimeter, area and diameter of the captured object can also be measured. In this context, the statistical methods used in image processing and the availability of these methods as well as the interpretation of the results are also important.

Although digital image processing is based on mathematical and probabilistic calculations, human visual perception also plays a significant and central role.

When images are transferred from the real environment to the digital environment through a camera, errors or distortions called "noise" may occur. Various statistical methods are utilized to correct these errors. Therefore, statistical image processing aims to provide more accurate results at the end of the analysis of the events and provides a great gain in terms of time.

During these operations, filters or masks consisting of mathematical functions or models are applied to the image. These methods, which are applied within the scope of image processing, allow the image to be interpreted more easily in visual and numerical aspects (Pitas, 2000).

With the advancement of technology, thanks to the computer hardware developed to meet human needs and the software that runs this hardware, studies in the area of image processing and interest in this area have increased gradually. However, how to take advantage of image processing methods has also been the subject of research (Asmaz, 2006). Thus, with the effective use of computers,

which have an important place in human life, an important point has been reached in the recognition of objects, the extraction of features and the classification of these objects. In the future, thanks to image processing and statistical methods, it is thought that there may be important developments that will facilitate human life in many areas such as astronomy, health, education, security, technology and industry.

In this study, after mentioning the basic concepts of image processing, it is discussed to determine some physical properties of the object whose image is taken by using image processing methods. In this context, the necessary literature review was made and an application using statistical methods used in image processing was included.

2. GENERAL INFORMATION

Image processing, which is one of the fastest developing areas in signal processing, and the methods used in image processing have been the subject of various research and studies in the world and in Turkey. As a result of these studies, many low-cost, safe and fast inventions that will facilitate human life have been signed.

Ghazanfari et al. (1997) classified pistachios into four quality classes: extremely large, large, medium and uncracked using image-based classification. In their study, the researchers used the grayscale histogram method and Fourier descriptors to determine the features and used hybrid decision trees and feed-forward neural network to determine the classification success.

Bennamoun & Boashash (1997), have applied automatic object recognition with image processing techniques in their work. From the image to which the edge detection algorithm was applied, the parameters of the specified objects were obtained and the object was defined.

Ünal et al. (1999) carried out quality control by using image processing methods in places where mass production is carried out in their studies. After the images obtained through the camera were processed with a suitable image processing software, measurements of the material were made automatically.

Fu & Liu (2001) have made an application of object detection and recognition based on image processing for autonomous vehicles. They used edge detection, Hausdorff distance transformation, coordinate determination and die comparison.

Özdemir (2004) conducted studies on the detection of rock fragments in the images obtained by numerical methods by image processing methods, performing dimensional analyzes and recording the results in tables and graphical representation. In order to image processing to obtain accurate results, an object whose size is known in advance is left in the environment where the rock fragments are located and the scale of the picture is created with this known value with the help of the scaling bar in the software. In this context; It is emphasized that properties such as the distance of the camera from the area being photographed and the angle of view are important in calculating how many centimeters of actual measurement corresponds to one unit of space in the picture.

Sinha & Fieguth (2006) have worked on the classification of images of underground pipes in terms of shape and structure.

Zhang et al. (2006) conducted a study on the classification of defects on the surfaces of sanded and polished objects by image processing. In particular, they have identified and classified the surface defects of products that are expected to be of aesthetic quality. In this classification process, in addition to the formal

characteristics of the errors; Discrete Cosine transform, Laws filters, Gabor filters and matrix-based statistical features were also utilized.

Edizer (2006) compared the actual measurements of rock fragments in the images with the digital measurements obtained using the "IMAGEJ" software. Thus, the size analysis of the mine grains is done easily and automatically by using image processing techniques and the data obtained are recorded.

Aslantaş (2006) conducted a study on calculating the ages of felled trees using image processing methods. In this study, the images taken from the tree section with the camera were divided into digital Red Green Blue (RGB) components, and the ring edges running parallel to each other were found and counted. With this study, acceleration and precision have been achieved in the counting of annual rings in tree sections.

Bal (2006) worked on obtaining features from images of an object using image processing methods. He used dominoes for the application of the research and used image processing techniques such as image enhancement, filtering, structural editing and segmentation for his study. According to the results obtained from the study, it is emphasized that appropriate lighting is the most important factor in extracting features from the image and that the resolution and structural properties of the object have an important place in image processing.

Bozkurt (2009), in his study, using the retina images he obtained; He touched on the separation of retinal vessels, optic nerves, optic disc and cup areas.

Mahmoud (2011) developed a system for the separation of cracked and closed pistachios. In his work, he used decision trees and fuzzy logic methods for both feature detection and classification purposes.

Ghezelbash et al. (2011) attempted to classify three Iranian pistachio species (Ohadi, Akbari and Kalle-Ghuchi) according to their open and closedness using thresholding and mathematical morphology methods.

Mutlu (2011) checked pneumatic cylinders using image processing-based ON-OFF control software in his study. For this, he made use of the threshold value method.

In his study, Yakut (2013) compared two different methods of object recognition using images of sign language. The first is to multiply the image by a weighted matrix and obtain a graph in the coordinate plane, and the second is to obtain a new graph by performing a 360-degree angular scan of the same image.

Ataş (2016a) has made the classification process with the virtual features of Siirt pistachios using image processing methods. Pistachios; It is divided into 6 classes as extra-large, large, medium, small, shell and closed. He used artificial neural networks in the classification and achieved a success rate of 83.33%.

2.1. Image

Image processing methods are methods that allow real-life three-dimensional images to be digitized using image sensing devices (camera, scanner, radar, x-ray, sensor, etc.), changing and improving their properties and structures, and performing analysis through these images. The basic structure of image processing is shown in Figure 1.

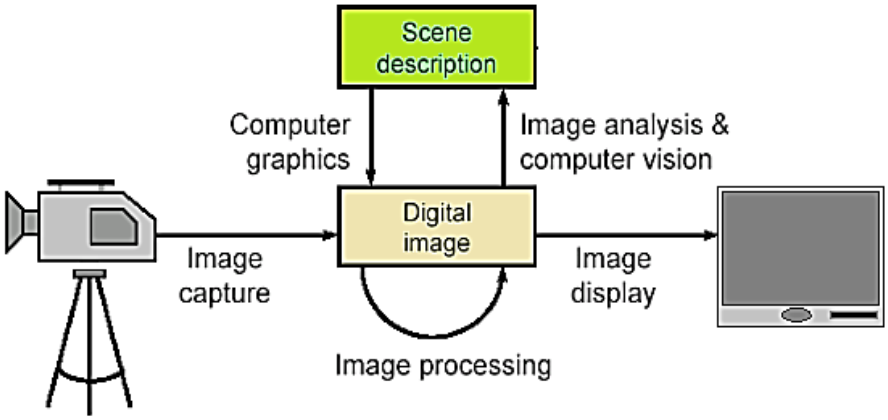

Figure 1. Basic structure of image processing (Gonzalez et al., 2004)

A digital image is a matrix obtained by digitally encoding a real 3D image with “r” rows and “c” columns. Each element of this matrix is called an image element or pixel, and this matrix consists of a total of rxc pixels. As shown in Figure 2, the numerical values contained in the matrix provide information about the color (λ), depth (z), time (t), brightness, resolution and number of pixels of the image (Young et al., 1998).

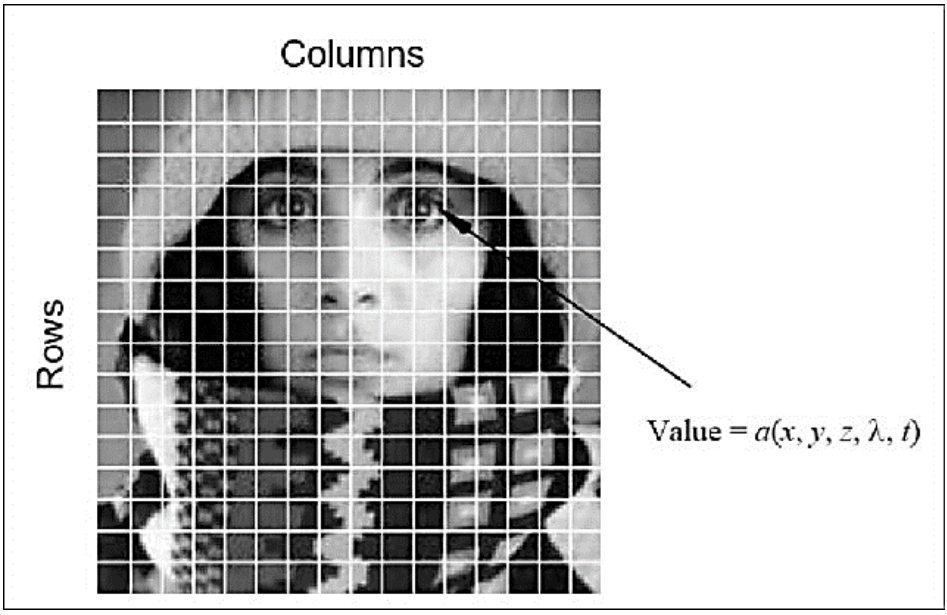

Figure 2. The elements that make up a digital image (Young et al., 1998)

2.2. Resolution

Resolution is described using the terms pixels per inch (PPI) or dots per inch (DPI). These terms are derived from the ratio of the number of pixels in the image to the physical size of the image. As the size of the matrix that makes up the image increases, the number of pixels of the resulting image also increases and the resolution of the image is better (Figure 3).

Figure 3. Actual size representation of different resolutions of the same image (Gonzalez, 2009)

The resolution of an image is described by the size of the matrix that composes it. The quality of the information to be obtained from an image with a high resolution is also higher. As shown in Figure 4, the square pixels become noticeable when looking closely at the image or when the image is enlarged and made to the same size (3.6 inches). If all the details in the image are sharp enough to be distinguished, it indicates that the resolution is high (Edizer, 2006).

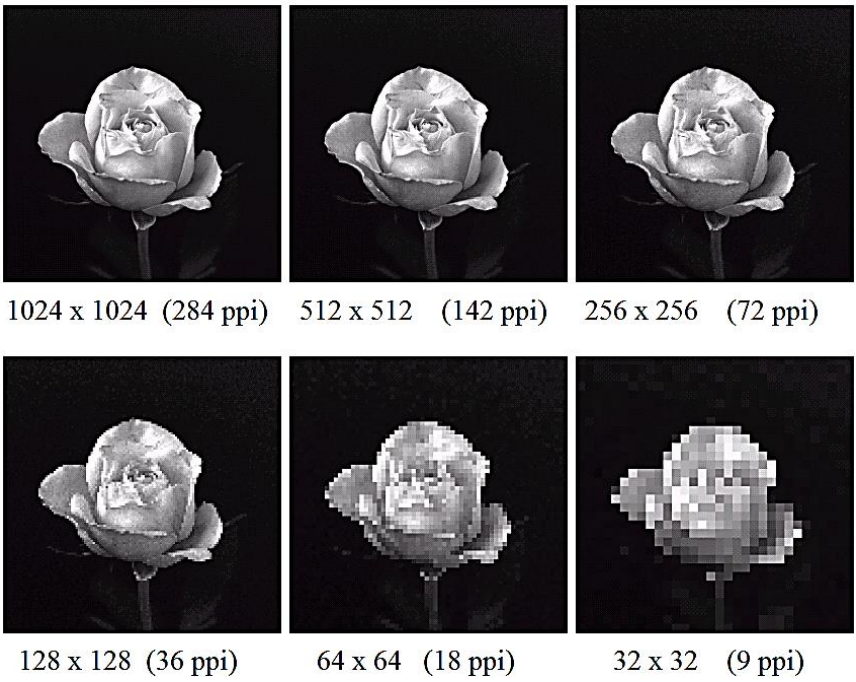

Figure 4. Same size representation of different resolutions of the same image (Gonzalez, 2009)

2.3. Contrast

The human eye has a limited capacity to distinguish values in hues close to each other. In other words, it can perceive the image differently according to local factors. Therefore, if the difference between low and high values in an image is small, the human eye may not be able to perceive the details in the image (Bellanger, 2000). Contrast in this context can be achieved by increasing or decreasing the difference between light and dark colors in the image (Göktaş, 2012). If the pixel values that make up the image are scattered in the range [0–255], this indicates that the contrast of the image is high (Figure 5), otherwise the pixel values are concentrated in a certain region, which can be seen to be low contrast when looking at the histograms of such images (Bellanger, 2000).

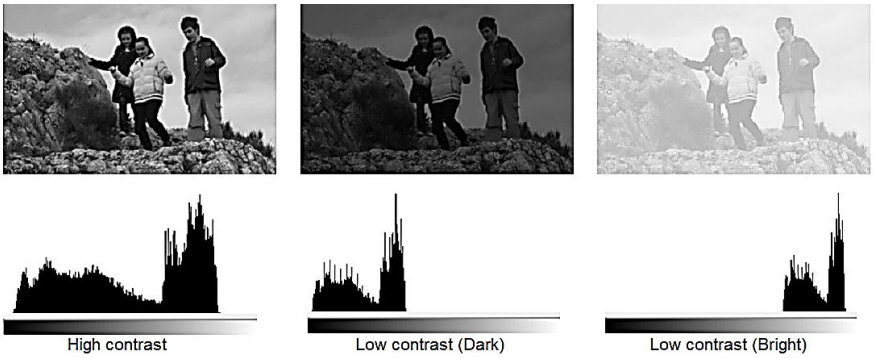

Figure 5. Joint representation of different contrasts (Göktaş, 2012)

Contrast is an important factor in image formation and perception by the eye. Although there is no difference between the pixel values in the image, the eye, which is affected by the difference of the surrounding pixels, can perceive the same pixels as if they were different. In Figure 6, although the squares in the center are of the same tone, they are also perceived as different due to the difference in tone of the surrounding squares. However, the computer encodes each pixel that makes up these frames to the same value.

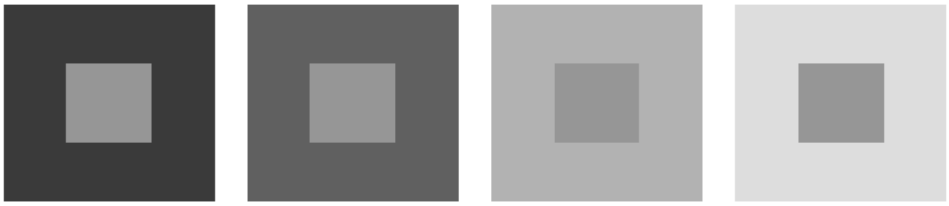
Figure 6. Examples of eye illusions (Gonzalez, 2009)

2.4. Brightness (Lightness- Darkness)

Brightness can be adjusted by adding a positive or negative value to pixel values in the range 0–255. If the added number is positive, the brightness of the image increases, and if it is negative, it decreases (Figure 7). The function of the original image is f(x,y); the function g(x,y) with modified brightness is written as "g(x,y) = f(x,y) + a (a: constant value)".

Figure 7. Light and dark states with the original image whose brightness has been changed (Gonzalez, 2009)

2.5. Representation of The Image With Colors

Color is a perception that occurs when light between 380 nanometers and 750 nanometers wavelengths reaches the eye. Radiations with a wavelength of less than 380 nanometers and high energy are called ultraviolet and low-energy radiations with a wavelength higher than 750 nm are called infrared. However, the electromagnetic Area that the human eye perceives as light or color only covers the range of 380 nm to 750 nm (Figure 8).

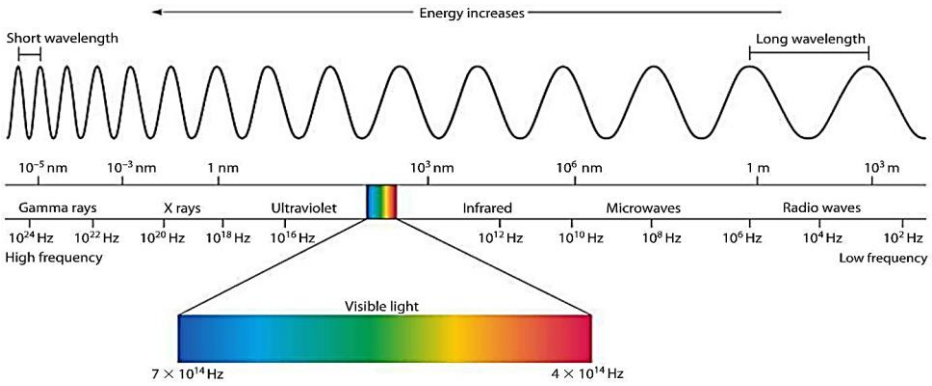

Figure 8. The electromagnetic spectrum (Anonymous, 2016)

The perception of colors takes place by reflecting the light by the objects and transmitting the object to the brain with the help of the eye. This perception is varied by the fact that light hits the substances and is partially absorbed and reflected. These are called color tones or colors. If all the color waves reach the eye at the same time, the color is perceived as white, and if none of them reach the eye, it is perceived as black (Metlek, 2009).

A color model (color space) is a way of representing colors and how they relate to each other. Today, there are many color models used for different purposes. 3 of them are shown in Figure 9 (Bushberg & Boone, 2011).

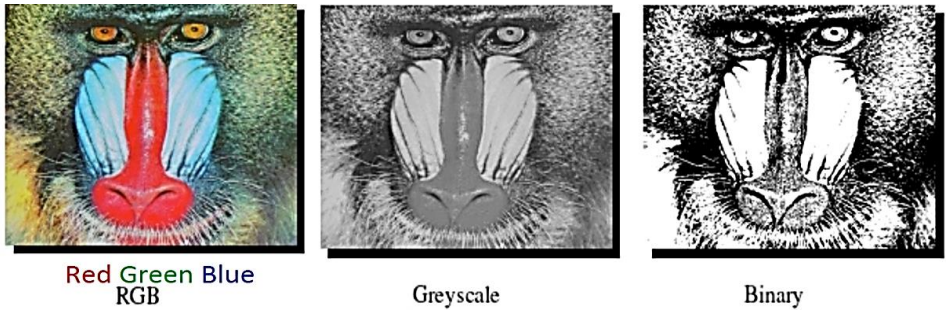

Figure 9. Color models (Karakoç, 2011)

2.5.1. Binary image

A digital image in which there is one of the possible values of 0 or 1 for each pixel in the image is called a two-tone image. Symbolically, a numeric value of 1 represents the color white, and a numeric value of 0 represents the color black (Figure 10). Each pixel occupies 1 bit of space. Therefore, the image matrix takes up a very small storage space. A binary image is the type of image that is most useful for working with, but it contains less information than other types (Russ & Woods, 1995).

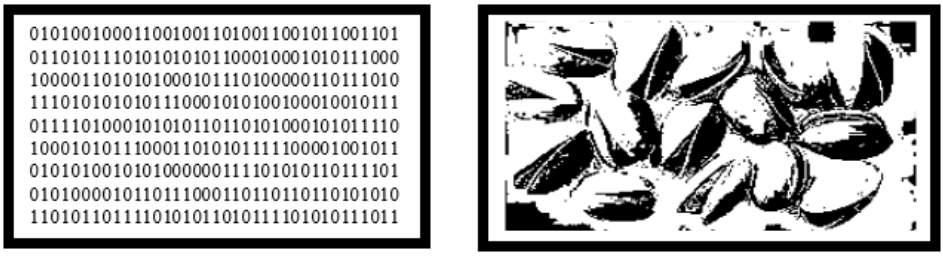

Figure 10. Binary (black and white) images and numeric values

2.5.2. Grayscale image

A grayscale image is created using tones between black and white. Symbolically, a numeric value of 255 represents the color white, and a numeric value of 0 represents the color black (Figure 10). All values between 0 and 255 represent shades of gray (Johnson, 2006). This gives the screen a grayscale image (Figure 11).

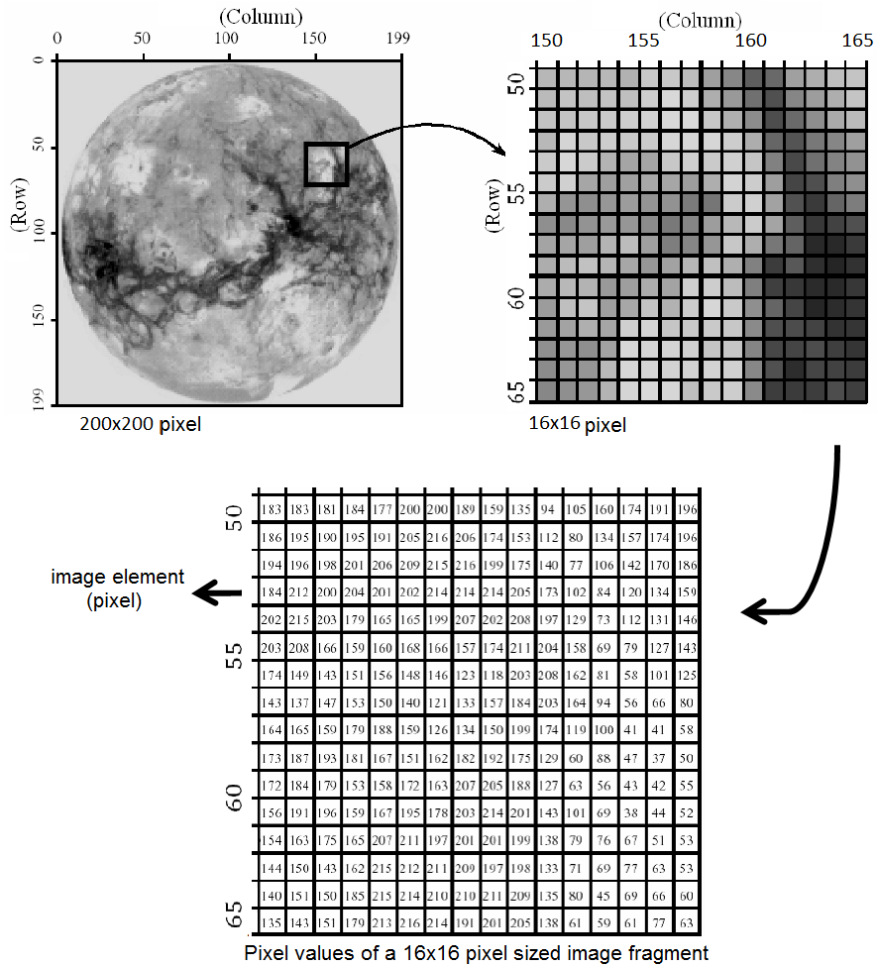

Figure 11. A grayscale image and the numeric values of the pixels in the image (McAndrew, 2004)

2.5.3. Color image

The RGB (Red-Green-Blue) color model has channels of 3 basic colors of red, green, and blue, and the color of each pixel is a combination of the shades of these three colors. So, it's a pixel; red, green and blue can be represented by a function consisting of a mixture of the basic colors in varying proportions. As shown in Figure 12, the image rxcx3 is a -dimensional matrix. Each color layer returns the ratio of that color for that pixel.

R(x, y): The red component receives a value between 0-255.

G(x, y): The green component takes values between 0-255.

B(x, y): The blue component takes a value between 0-255.

F(x, y) = [r(x, y) g(x, y) b(x, y)]

In the RGB color space, millions of different colors can be obtained by using different ratios of the three basic colors.

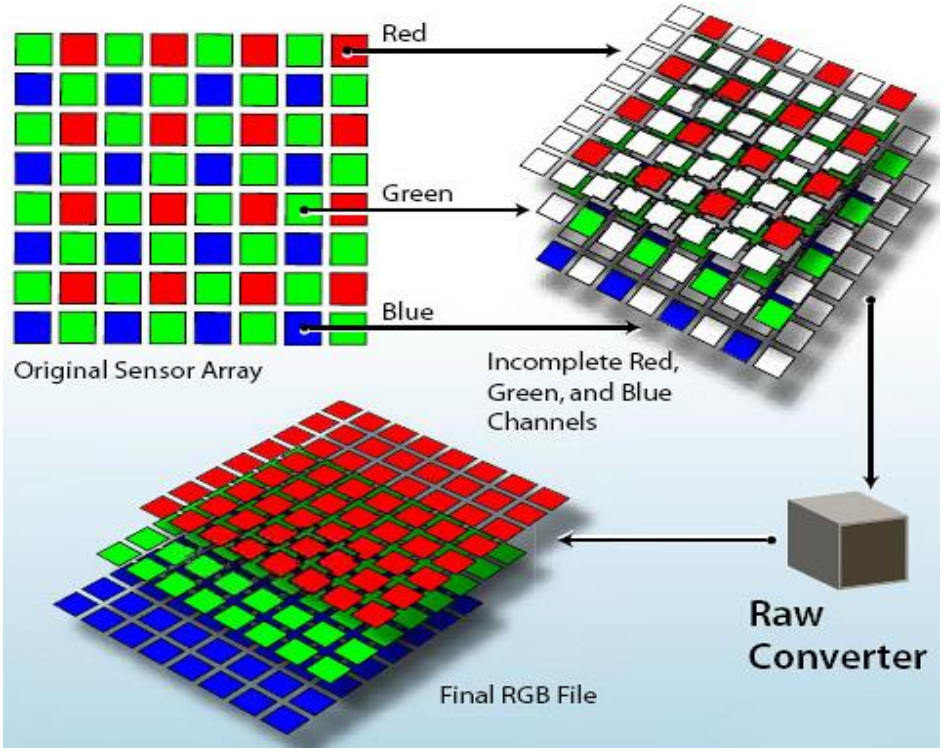

Figure 12. Representation of basic colors in 3 layers (Sharma & Dadwal, 2015)

A 3-dimensional cube with red, green, and blue colors on its axes (Figure 13) can represent the RGB color space. At the origin is black color; at the opposite end is white color. The grayness scale is located above the diagonal, which combines black and white (Crane, 1996).

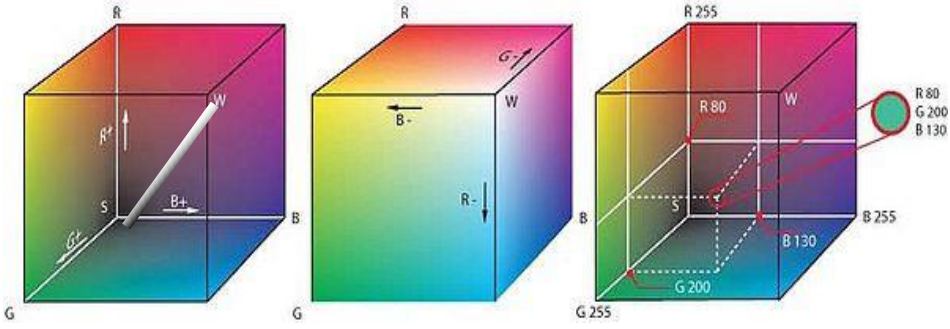

Figure 13. Cubic representation of RGB space (Okur, 2015)

Pixels where all three components receive a value of zero are colored black (0, 0, 0) and pixels where they receive a value of 255 are colored white (255, 255, 255). If all three components receive equal values between 0 and 255, then grayscales from black to white are obtained. If the components are different from each other, one of 16.777.216 different colors is obtained.

2.5.4. Conversion of color image to grayscale image

Converting a color image into a gray image is essentially reducing the 3-dimensional color space to a single dimension. Therefore, each pixel, which was previously composed of three components, is represented by a single value in the range [0-255] (Mutlu, 2011).

Reducing the image to the grayscale is a method used for the image processing algorithms to work more comfortably, and this reduction process differs according to the image processing algorithm to be applied (Yakut, 2013). There exist three methods for converting a pixel consisting of an RGB color model to a grayscale pixel (Figure 14).

First, of the red, green, and blue colors that range from 0 to 255, the largest and smallest ones are averaged and treated as the grayscale color of the new pixel.

Second, the mean of the base colors red, green, and blue that make up the colored pixel and take values from 0 to 255 is considered the grayscale color of the new pixel.

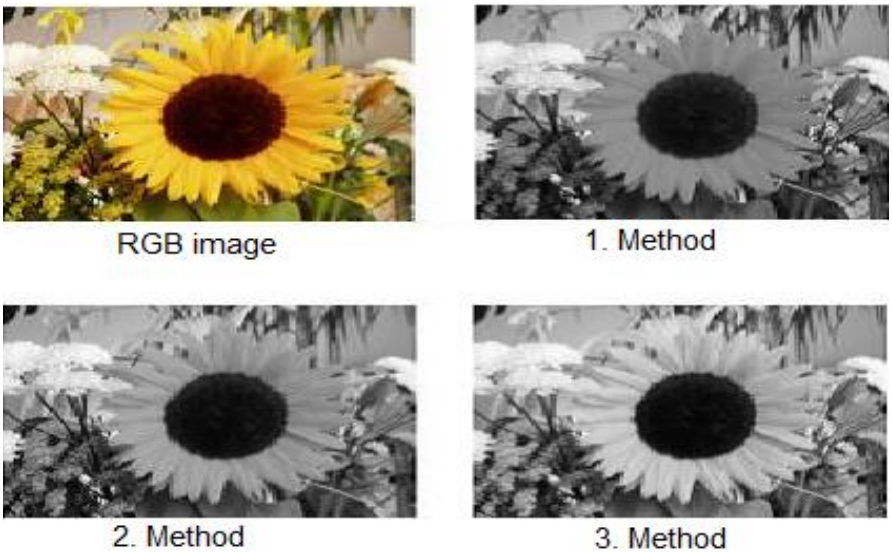

Figure 14. Grayscale conversion of RGB image by three different methods (Doğan, 2016)

Third, human perception is also taken into account when finding the Mean value. Because the human eye is more sensitive to some colors than others. For this, each color is multiplied by its predetermined weight (0,21 R, 0,72 G, 0,07 B). Then the weighted mean of the three primary colors is taken. This gives the value (Doğan & Ataş, 2015) of the new grayscale pixel.

2.5.5. Conversion of a grayscale image to a binary image

The threshold method is used when converting an image from gray [0-255)] to a binary image (0,1). When determining the value of the limit to be determined as the threshold, it should be taken into account that the information to be obtained from the image is optimal. The value of each pixel is compared to the predetermined threshold value. Pixel values less than the threshold value are subtracted to 0 and pixel values greater than the threshold value are subtracted to 1 to create a binary image (Doğan & Ataş, 2015) consisting only of black and white colors. After the grayscale image is converted to a binary image, features of the objects in the image can be extracted using different techniques.

2.6. Noise and Filtering Methods

Many defects occur in images due to incorrect image recording by digital image recorders, incorrect lighting in the environment, sensor or lens errors, motion blur and errors that occur during the image storage phase. These disturbances are called noise. The purpose of image processing filters and masks is to improve the image, to increase its authenticity (Young et al., 1998).

Each element of the numeric image matrix is passed through these filters and the value of each cell is recalculated. When calculating this new value, the values (Arslan, 2011) of the surrounding cells are also taken into account.

2.6.1. Types of noise

Salt and pepper noise: It is the noise generated by black and white pixels randomly scattered over the image (Figure 15).

Impulse noise: It is the noise generated by white pixels randomly distributed over the image (Figure 15).

Gaussian noise: It is the noise generated by black and white pixels randomly scattered over the image (Figure 15).

Figure 15. An example image of noise types (Anonymous, 2019)

2.6.2. Mean filtering method

The Center filter consists of square matrices made up of odd numbers, such as 3x3, 5x5 or 7x7, that center the pixel being worked on. The filter matrix passes over all the pixels. Each pixel in the image is averaged with neighboring pixels, and the resulting new value is written as the value of that pixel. The larger the size of the filter, the more details in the image are lost and the lower the resolution of the image. This method is particularly effective for removing gaussian noise.

With Mean filtering, noise in the image is eliminated and sharp neighborhoods between pixels are smoothed out. However, this smoothing causes sharp details to be lost and blur increased, which is one of the negative aspects of the Mean filter (Figure 16). In this case, the resolution of the image decreases after the application of the Mean filter. However, this problem can be eliminated by different methods used in image processing (Young et al., 1998).

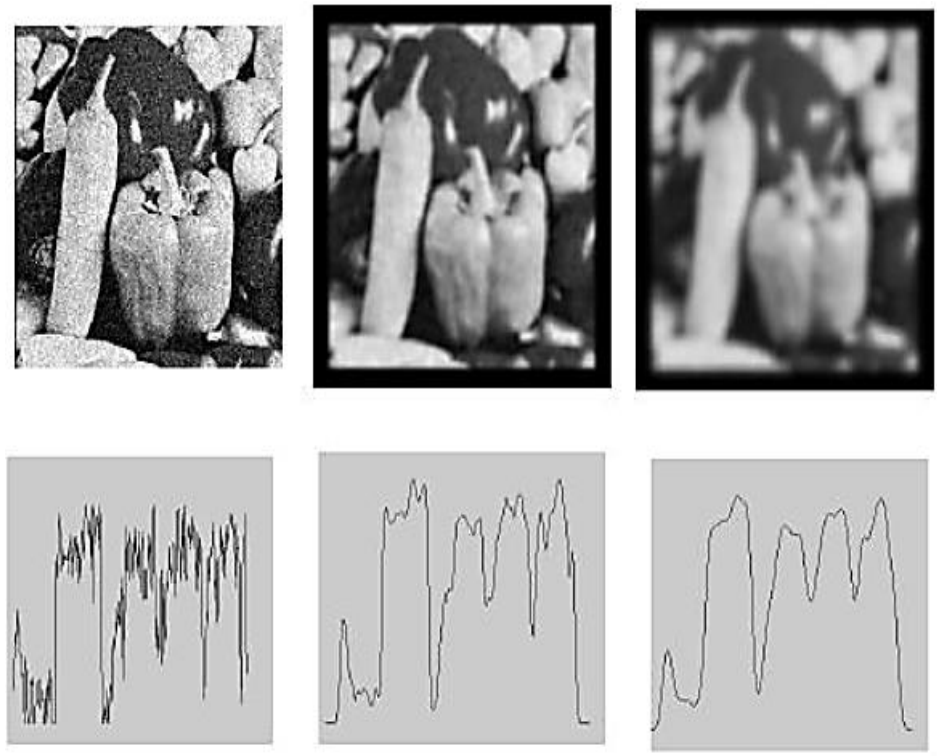

Figure 16: Twice mean filtered image (Anonymous, 2019)

2.6.3. Median filtering method

The Center filter consists of square matrices made up of odd numbers, such as 3x3, 5x5 or 7x7, that center the pixel being worked on. The filter matrix passes over all the pixels. Each pixel in the image takes the median value with its neighboring pixels, and the resulting new value is written as the value of the pixel (Figure 17).

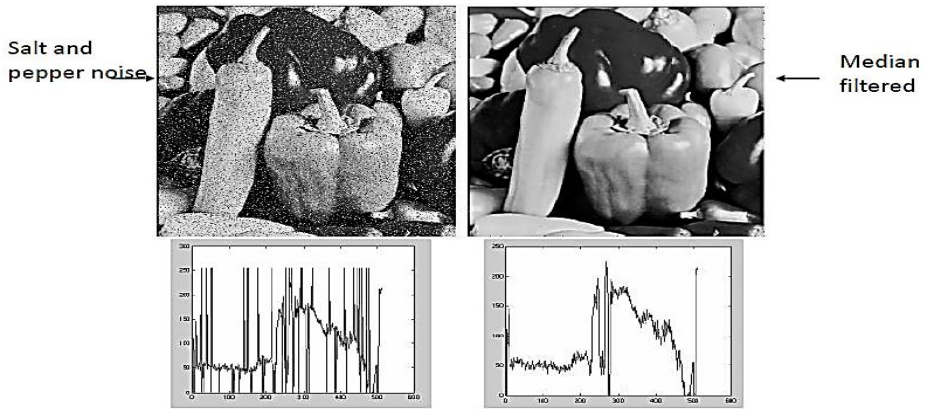

Figure 17. Example of salt and pepper noise removal with median filter. (Anonymous, 2019)

If the mean and median filters are compared, it can be seen that the median filter is a more effective filter for removing "salt and pepper noise" and "impulse noise", as shown in Figure 18 (Qidwai & Chen, 2009).

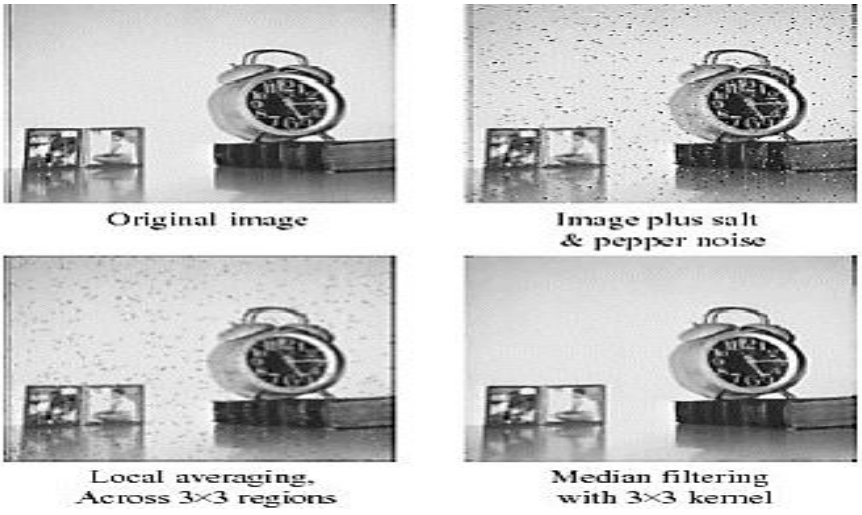

Figure 18. Comparison of processing an image with salt and pepper noise with a 3x3 median filter and a 3x3 mean filter (Anonymous, 2003).

2.7. Image Thresholding Method

As with the conversion of a grayscale image to a two-color image, the thresholding method sets a threshold value before the image is subjected to the thresholding process. In determining the threshold value, the desired result from the image and the condition of the original image play a major role. Pixels with a

grayscale value higher than the threshold value are assigned a numeric value of 1, and pixels with smaller values are assigned a numeric value of 0, making the image simpler black and white (binary). As shown in Figure 19, the thresholding method is used to distinguish objects in the image from the background and other objects.

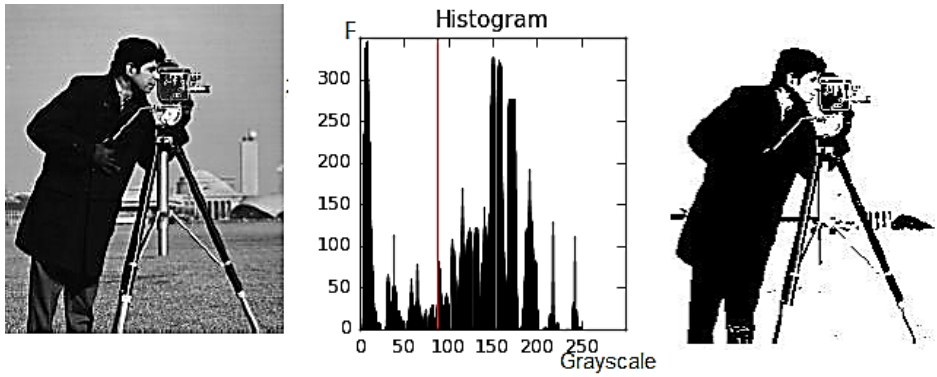

Figure 19. Pre- and post-thresholding images and image histogram (McAndrew, 2004)

For images with multiple objects with different hues, the threshold value is also multiple. This separates each object from both the background and the other objects. How many threshold values to determine is decided by looking at the distribution in the histogram of the image (Figure 20).

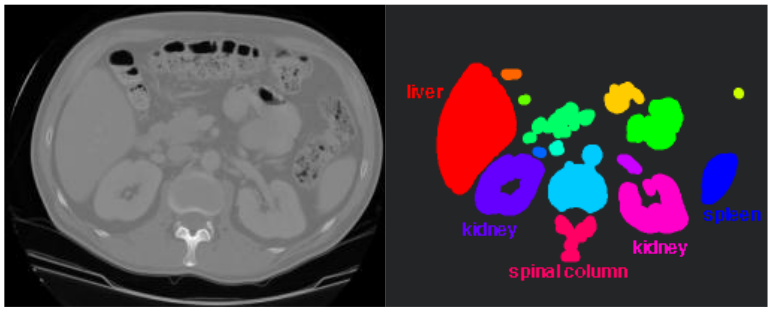

Figure 20. Object determination using multiple threshold values

2.8. Mathematical Morphology

Mathematical morphology is the method used to perform operations and analyzes related to geometric objects. Mathematical morphology, which is basically based on the set theorem, also forms the basis of morphological image processing. With mathematical morphology, which concentrates on the concepts

of continuity and space by characterizing the geometrical and topological properties of objects in the image; operations such as image repair, texture analysis, particle analysis, shape analysis, skeleton determination, gap reduction and edge determination can be performed with ease (Serra, 1982).

The most commonly used mathematical morphology operators are; erosion, dilation, opening and closing. Along with these, Mathematical morphology operators such as shrinking, thinning, tricking, skeletonization , pruning and distance transform are also used.

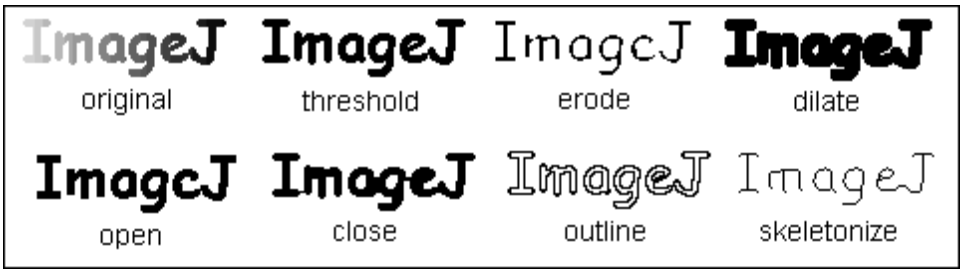

Figure 21. Mathematical morphology operators

To be able to apply these operators to an image, you need a group of pixels that are used as structuring element and pass over each pixel in the image. structuring element can be of different shapes and sizes. in determining the structuring element, the condition of the image and the desired operation play an important role (Acar & Bayram, 2009).

2.8.1. Erosion

It works to eliminate protrusions that attract attention as redundancy in objects within the image and bridges between objects that appear to be glued together. As a result, both the gaps between groups of pixels are reduced and some unwanted noise in the background of the image is removed (Edizer, 2006). As shown in Figure 22, the original image, which previously had white striped noise, is cleaned of these noises and protrusions in the groups of pixels that make up the letters after abrasion is applied.

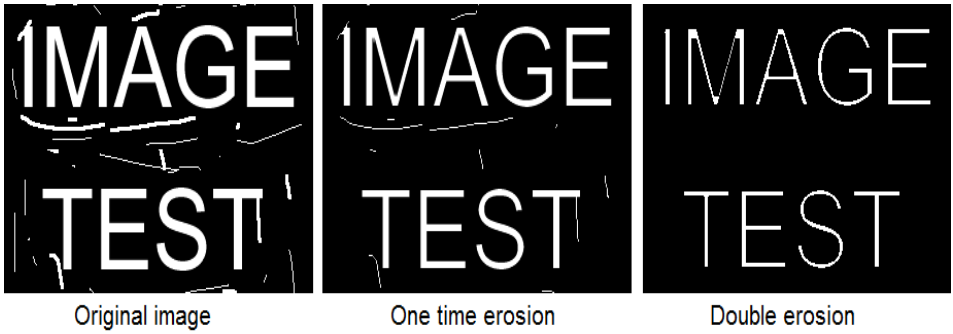

Figure 22. Implementation of the erosion operator twice

2.8.2. Dilation

The main effect of the dilation operator is that it expands and magnifies objects in the image. Thus, the gaps and deficiencies in the objects are completed (Figure 23). As a result, some unwanted noise on the object is removed (Gonzalez et al., 2004).

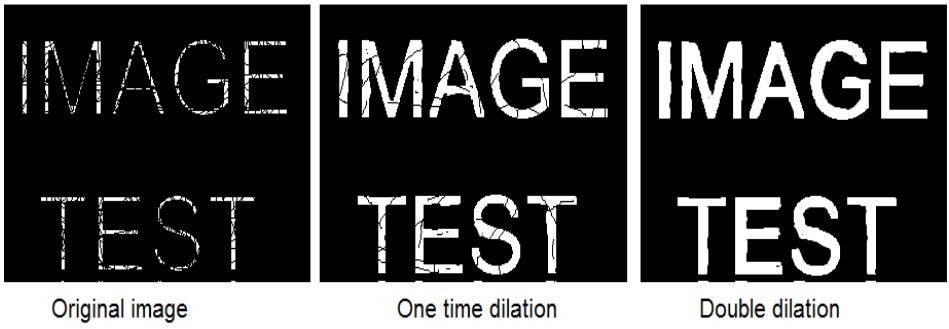

Figure 23. Implementation of the dilation operator twice

2.8.3. Opening

Depending on the problem in the image or the desired result from the image, different combinations of wear and expansion can be applied. For these applications, the same configuration element can be used each time or different configuration elements can be used depending on the need. The aim is to soften the image by removing noise both on the object and in the background (Bal, 2006).

The operator applied by first abrasion, then expansion is called Opening. Objects that are freed from external noise and excess due to abrasion but shrink due to thinning are restored to their original dimensions by applying the expansion operator (Figure 24).

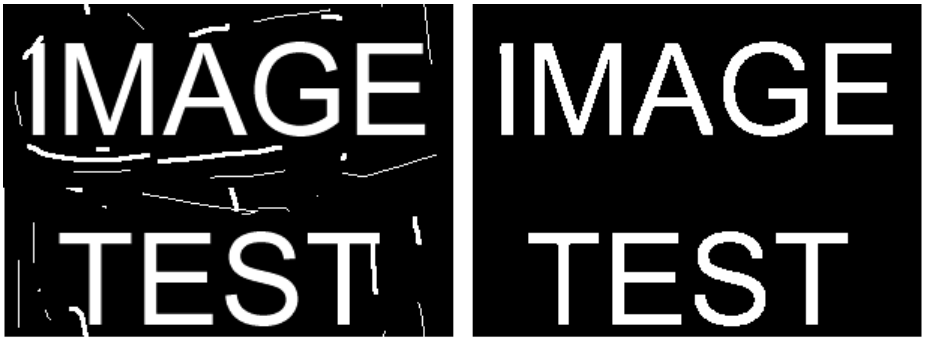

Figure 24. Opening with double erosion followed by double dilation processes application.

2.8.4. Closing

The operator applied by first expanding and then abrading is called "Closing". Noises and gaps on the object are removed after the expansion application. However, due to the expansion, the object that is larger than its original size is etched back to its former state (Figure 25).

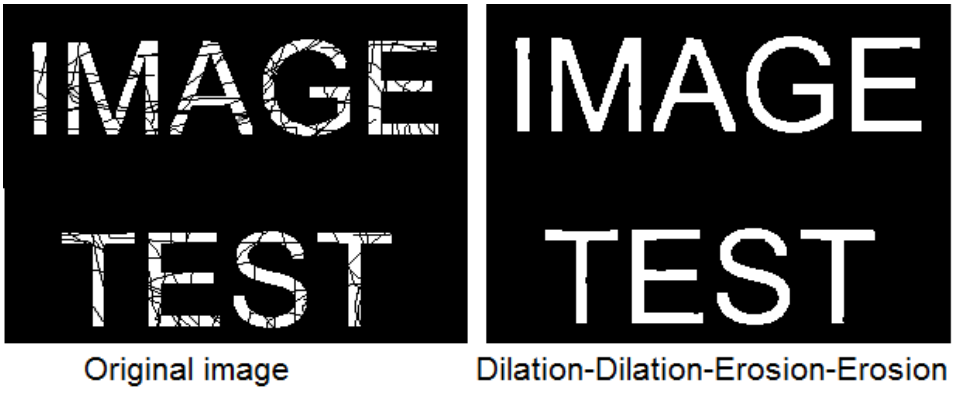

Figure 25. Closing with double dilation followed by double erosion processes application**.**

2.9. Histogram Equalization (Contrast Adjustment) Method

In image processing, measures such as mean, standard deviation, mode and range are basic measures of the distribution of pixel values in the image, and the histogram plot of the image contains frequency information about the pixel values (Russ & Brent Neal, 2016). Pixel values (0-255) are on the horizontal axis, and the frequency of color tone is on the vertical axis.

The image histogram contains information about the frequency of the pixel values that make up the image, but not the location of these pixels. In addition, the distribution of pixel values provides general information about the resolution, brightness and contrast of the image. In the light of this information, the threshold value to be applied can be determined or various interpretations can be made about the image (Mutlu, 2011). Image contrast can be adjusted using the values in the histogram chart to make the image clearer. For this process, the values in the histogram need to be more discrete and uniform (Figure 26). Thus, it can be seen that the image becomes more pronounced.

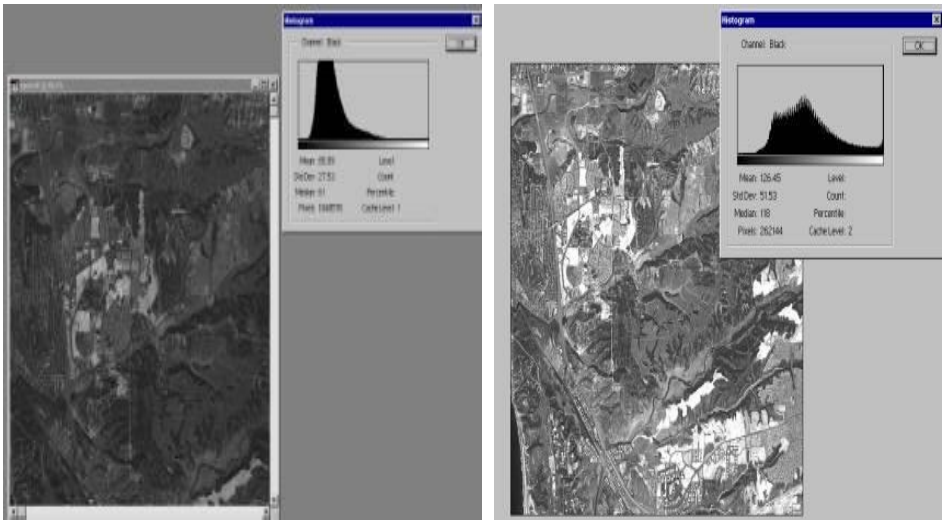

Figure 26. Example image and histograms before and after contrast adjustment (Perihanoğlu, 2015)

The lowest and highest pixel values in the histogram are determined and the pixel values are stretched provided that they are in the range of 0-255. That is, the range value is kept as wide as possible (Marchand-Maillet & Sharaiha, 1999). This expansion of the histogram makes the dark pixels darker and the light pixels brighter, increasing the contrast of the image and making it more open to visual interpretation (Göktaş, 2012).

2.10. Image Mapping Method

Image matching can be defined as the process of detecting another smaller image in an image (Karakoç, 2011).

Mapping is done using similarities in control points such as points, edges, and vertices that match each other within the two images to be compared. Thus,

similar images in another image can be detected using a template image (Ding et al., 2001).

In an image, a master image matrix of the object to be searched in the image is first created. The pattern image is then searched everywhere possible in the source image and investigated for the presence of similar objects in the image (Figure 27).

Figure 27. Template and target image to search for the pattern in

The features of the master image and the features in a certain part of the source image are expected to be close to each other. In this method, where accuracy and speed are important factors, if the pattern image and the source image match, the position of the matching part is determined (Karakoç, 2011).

Image mapping methods; It can be examined in three basic categories as Area-based, detail-based and relationship-based

2.10.1. Area-based methods

These methods are applied by using various similarity measures based on pixel values for the two images to be compared (Çavdaroğlu, 2013).

The matrix of size r x c of the desired master image in the source image is compared with all possible sections of the same size as itself. A similarity measurement process is performed for each position where the mold image is hovered. Whether the similarity measurement found is acceptable or not is decided according to the predetermined threshold value.

2.10.1.1. Correlation method

Correlation measures take values in the range [0,1]. The matrix of the master image, which is moved in all possible positions starting from the first position, is correlated with the image matrix in the relevant region of the source image. Based on the correlation value found, it is decided whether the mapping is appropriate or not. If the correlation measurement is 1 or close to 1, it can be said that there is a linear similarity between the two image matrices. If the correlation value is close to 0, it is decided that there is no similarity, that is, the image sought is not included in the source image (Figure 28).

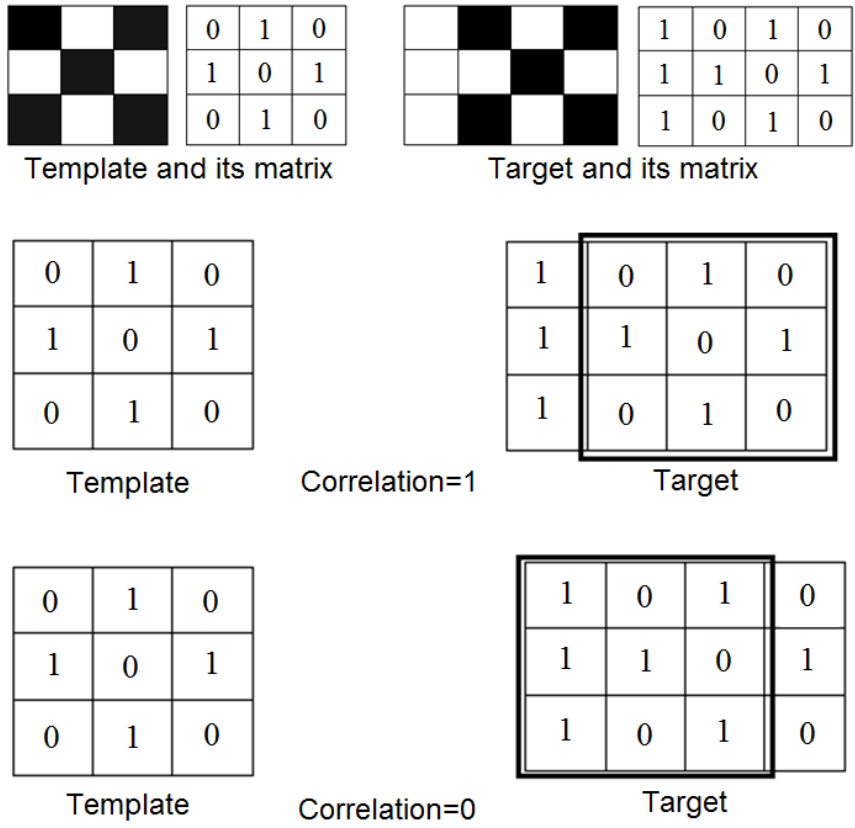

Figure 28. Binary pattern image and two possible state source images

For grayscale images with different shades, if the pixels of the matrix of the source image matrix, which is the same size as the pattern image and the pattern image, are multiples of each other during image matching, the correlation is high and one of the images is interpreted as darker or lighter than the other (Figure 29).

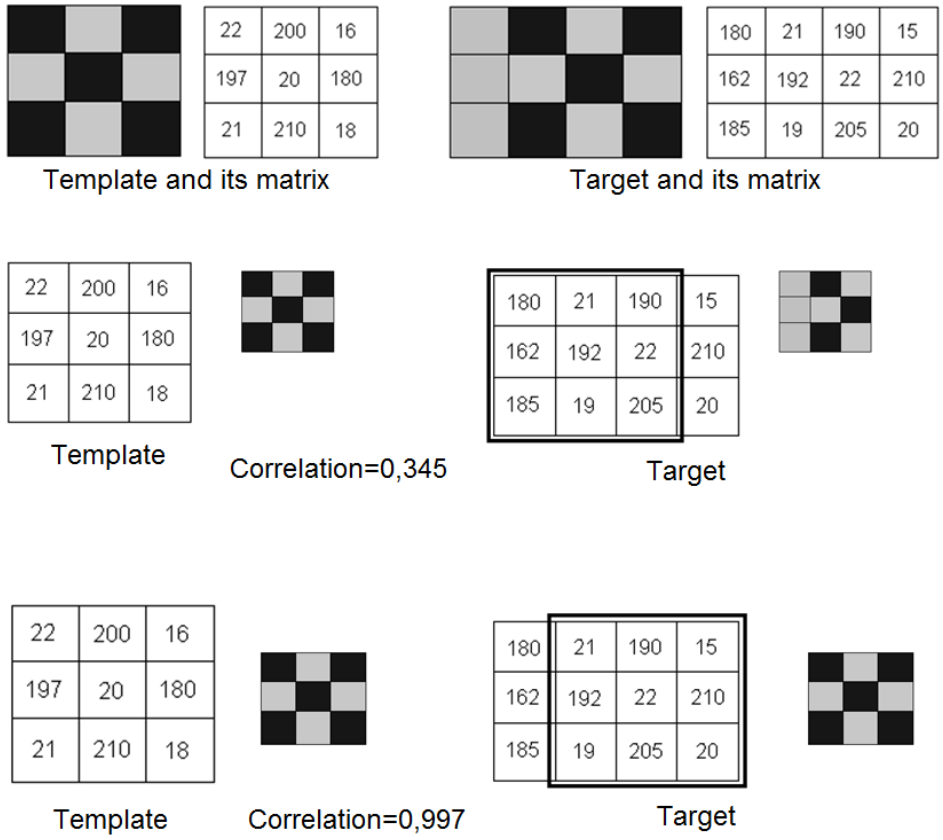

Figure 29. Grayscale pattern image and two possible state source images

2.10.1.2. Least squares method

During the image matching process, some geometric (object size, structure, distance, and change over time, etc.) and radiometric (illumination, reflectivity of the object, and characteristics of the sensor, etc.) differences between the two images to be matched may occur (Figure 30). Because of these differences, the simple linear correlation method in image mapping may not work well enough. However, in the least squares method, when mapping the image; Some additional information is used, such as accuracy assessment, weight values of observations

and error amounts, so that radiometric and geometric differences can be eliminated.

The basic logic in the least squares method is to measure the gray value differences between the lookup window and the pattern. Geometric and radiometric corrections are also applied during this process (Çavdaroğlu, 2013).

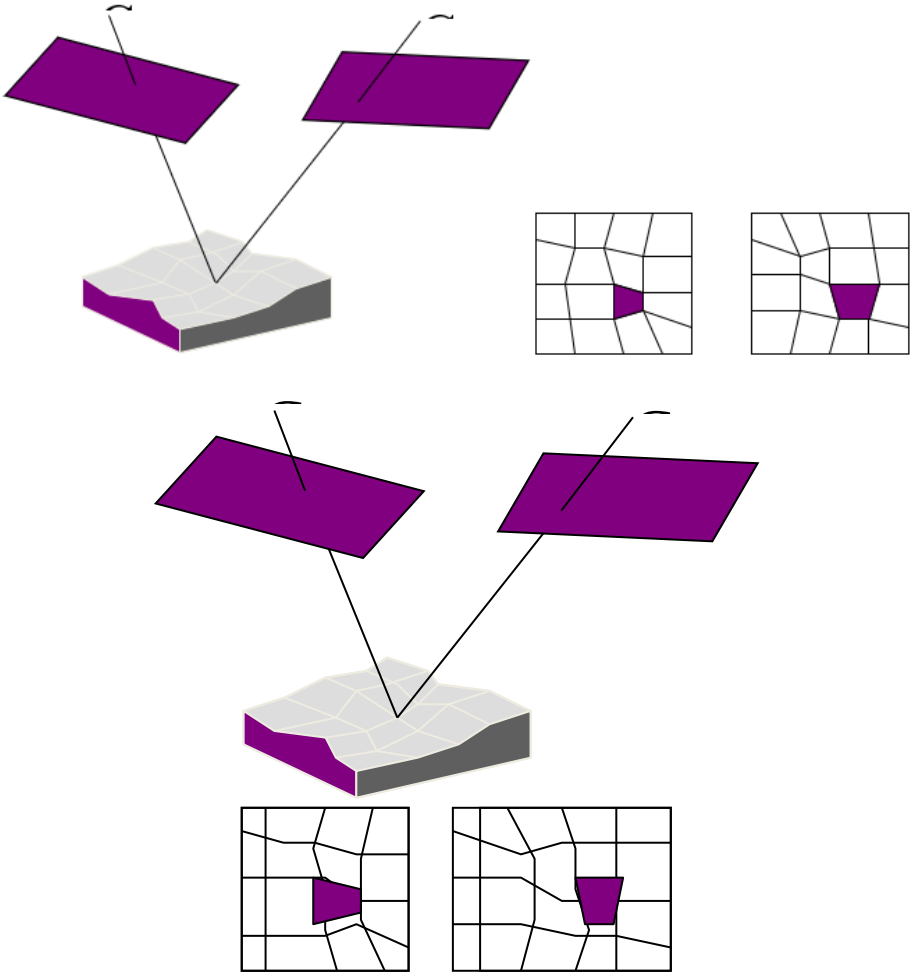

Figure 30. Example of matching that occurs despite differences

2.10.2. Object and detail-based methods

Unlike area-based matching operators that match based on pixel values in the image, object-detail based matching methods are based on details such as points, edges and areas. In low-contrast images, various features are extracted using algorithms such as attrition, segmentation, and edge detection. Removing features

is a critical phase of image mapping. The features that are extracted should be distinctive and the optimum number so that the mapping process can be simpler, more accurate and faster. As a result, these features are compared and matching is performed (Çavdaroğlu, 2013).

Instead of using an entire image in an image map, features of the image, such as points, corners, edges, and areas, make up the image's set of details. The feature and method to be used in the matching process varies according to the problem (Gonzalez et al., 2004).

If no logical or algorithmic drill-down method can be found for mapping, one of the dimension reduction methods, such as principal component analysis, can be used (Duda et al., 2001)

2.10.2.1. Point mapping

Detail (correlation) points in the image are points that are distinguishable within the image and are not affected by geometric and radiometric differences. The corresponding point detection operators are used to find them. These detailed points are matched with density-based matching methods (Figure 31).

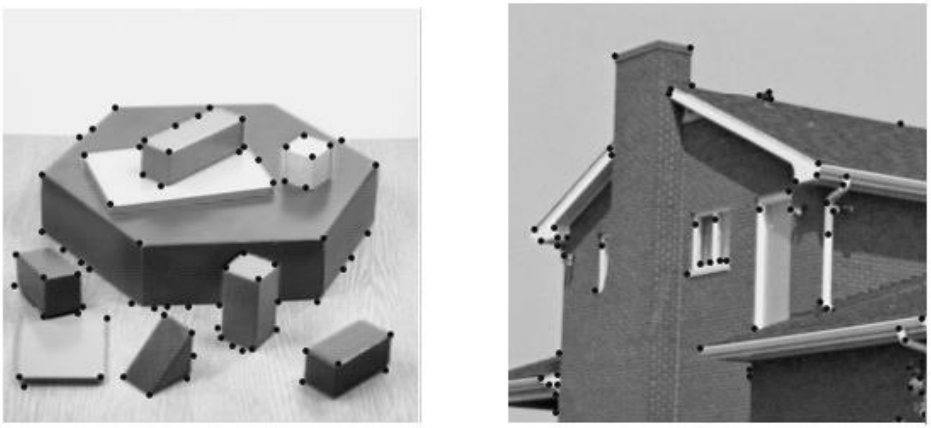

Figure 31. Example of point mapping (Çavdaroğlu, 2013)

2.10.2.2. Edge–vertex mapping

Places in an image where gray values change abruptly form the edges and corners of the object. The edges of objects in an image are determined using the edge detection or line removal operators. The edges found are mapped (Figure 32).

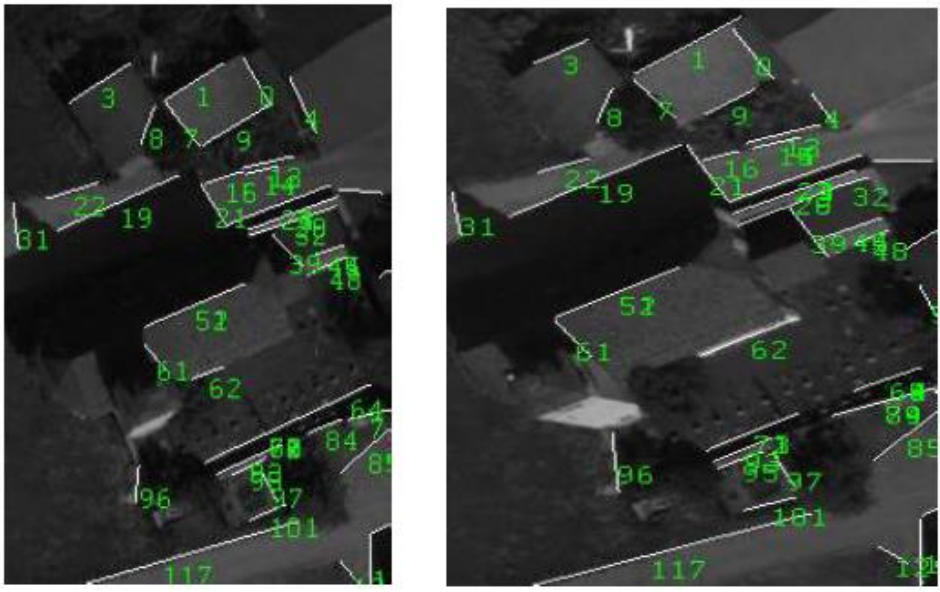

Figure 32. Edge (Corner) mapping example

2.10.2.3. Area - shard mapping

The area and fragments in the image are extracted and mapped with operators such as thresholding and segmentation (Figure 33).

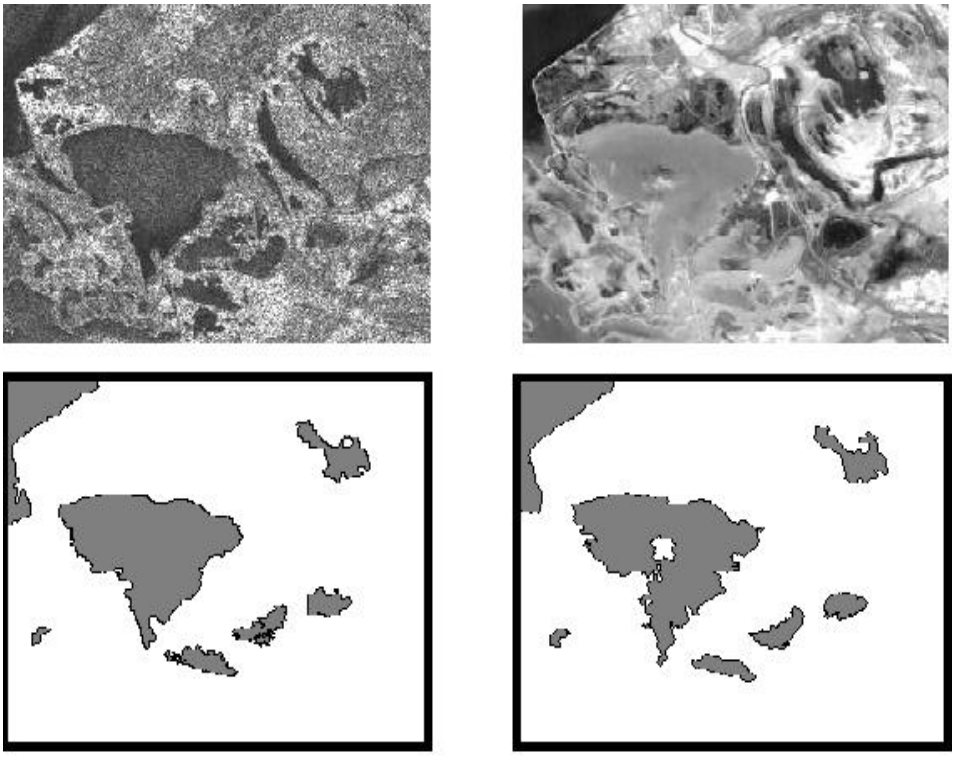

Figure 33. Example of Area (fragment) mapping

2.10.3. Relational methods

Relationship-based methods, on the other hand, are based on the use of structural links between the features of the details obtained from the image such as points, edges, corners and areas. In other words, these features are not considered separately, but as a whole, and the mapping is done in this way (Çavdaroğlu, 2013).

Since point features and other simple features cannot represent the entire image, geometric and symbolic relationships between images must be used (Ok et al. 2010).

2.11. Detection of edges in the image

In an image, the color transitions that form the boundaries between objects and the background are called edges. With edge determination, which is one of the first steps of image analysis, objects are distinguished from both each other and from the background.

Compared to image thresholding, edge detection does not identify all pixels of the object, but only the pixels belonging to the boundaries of the object,

filtering out the excess information to reduce the burden on subsequent processing steps (Okur, 2015).

The purpose of edge detection is to detect and sharpen rapid color transitions at pixel values in an image. this determines the boundaries of the objects in the image, which plays an important role in detection the features of the objects (Çelik, 2014).

In the edge detection process, due to low contrast, incorrect lighting, optical and geometric problems, the edges may not consist of sharp transitions but may be smooth transitions (Figure 34). This makes the edge detection process difficult.

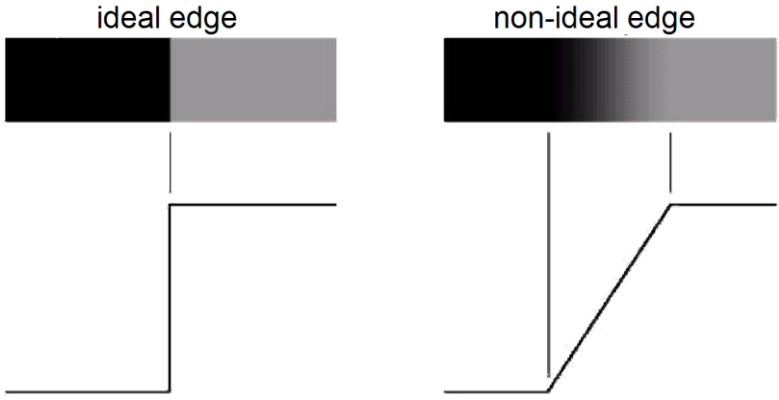

Figure 34. Grayscale representation of ideal and not-so-ideal edge models

Various edge detection algorithms have been developed to address these challenges and problems. The most commonly used edge detection algorithms are Canny, Prewitt, Sobel, Robert, Laplace and Log filters. In Figure 35, Canny, Sobel and Laplace edge detection filters are applied to a grayscale image and the results are given (Gonzalez et al., 2004).

Figure 35. Edge detection algorithms applied to a grayscale image (Okur, 2015)

Detection of edges in an image consists of three basic steps (Çankaya, 2013):

- Remove noise from the image: Various noise cancellation filters are used to remove noise so that the edges in the image are not affected.
- Edge reinforcement: In the image, edge-forming regions are detected using filters such as enlargement, contrast enhancement and thresholding with edge detection algorithms.
- Detection of edge in the image: Determine whether the regions identified as edges in the output of the process are actually edges.

3. MATERIALS AND METHODS

3.1. Material

In the study, 50 Siirt Pistachio Nuts (*Pistacia vera* L. cv. Siirt) were used as application material. Ziplock bags were prepared for each of these and each pistachio was given a sequence number, which was its identification number for the duration of the study. In addition, a folder with the same numbers as the bags was opened for each pistachio sample on the administrator computer for image processing. Measurements were taken from these pistachios as described in the method section and these measurements were used in the calculations.

3.2. Method

3.2.1. Obtaining of real data

In order to estimate the actual measurement values from the values obtained by image processing and to demonstrate the predictability of this, the weight (g), length (mm) and width (mm) measurements were taken from the physical real features of each pistachio (Figure 36).

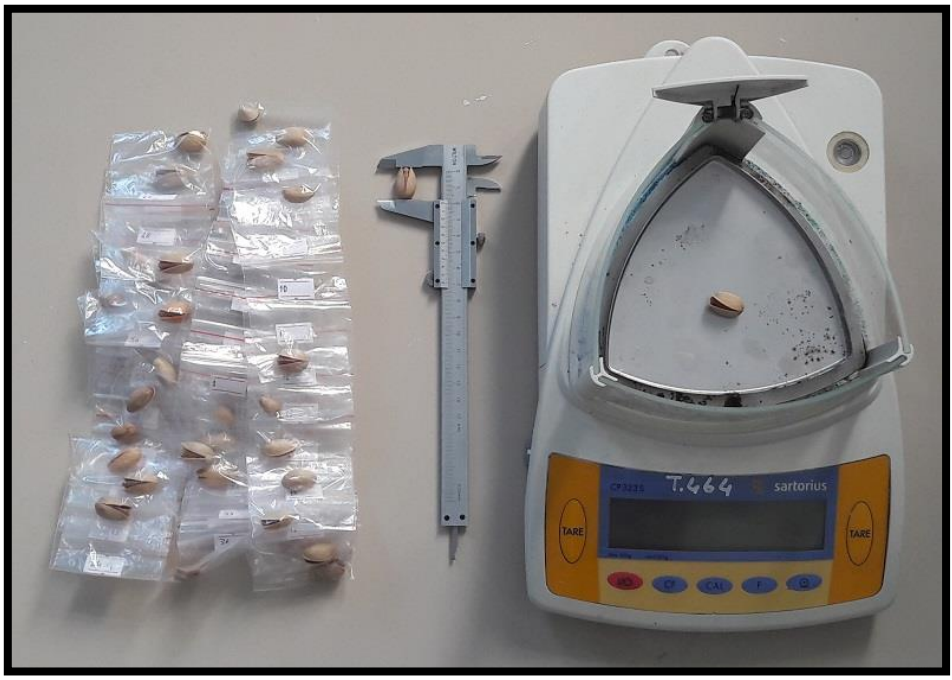

Figure 36. Measurement of real data on pistachios

A balance with a measurement accuracy of 0,001 g was used for weight. Each pistachio was weighed and the resulting measurement was recorded in the folder containing the information about the relevant pistachio.

A caliper with a measurement accuracy of 0,1 mm was used to measure the length and width of the pistachios. The measurements obtained for the length and width were recorded in the folder where the identification number of the same pistachio was written.

3.2.2. Obtaining of images

The imaging layer of the pistachio sorting machine was used to take the image. Each pistachio is left in a glass pipe with an inner diameter of 16 mm in the machine to take an image. The pistachios moving down through the glass pipe were imaged by means of cameras located below and placed to see the center at a 120-degree angle. Thus, 3 images of a pistachio that can be seen from different angles were obtained. This process was repeated 100 times for each pistachio sample to improve measurement accuracy. Thus, 300 images were obtained for each pistachio and these images were saved in the corresponding folder (Figure 37).

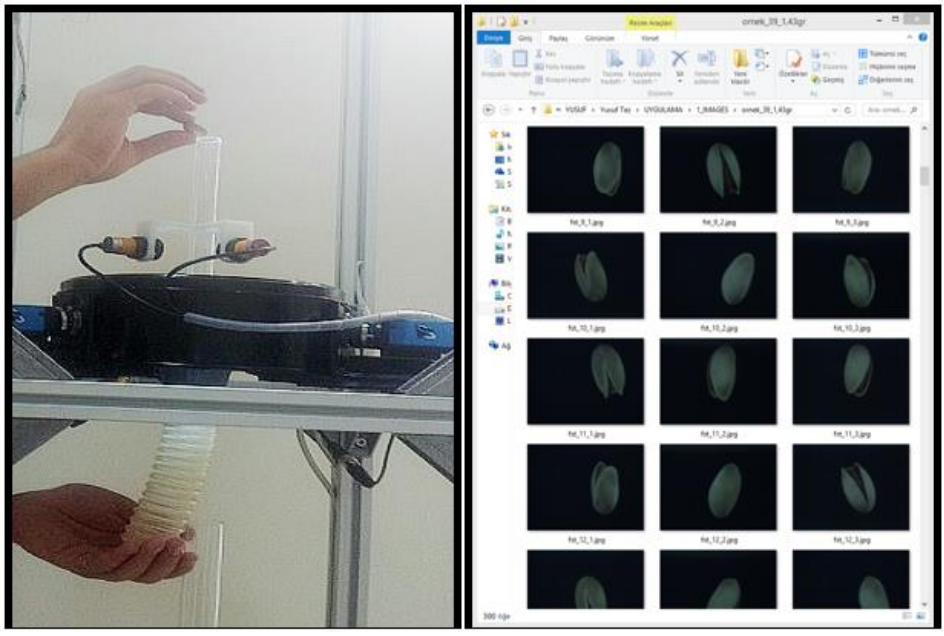

Figure 37. The process of obtaining images

3.2.3. Obtaining of virtual features

Using image processing techniques, obtaining numerical data about the physical properties of an imaged object is called feature extraction. Instead of dealing with the whole image at hand; operations are performed on an object-by-object basis using techniques such as thresholding, edge detection, and image mapping.

With feature extraction, the size of an image that is actually complex is reduced to simple properties (Figure 38). Accurate feature extraction is crucial for the performance of image analysis (Okur, 2015).

Figure 38. Image with some features extracted automatically

For each pistachio to be used in the study; A total of 6 features were utilized: perimeter, crack, area, width, length, and circularity. A software library called Open Cezeri Library (OCL) was used to extract these features (Ataş, 2016b).

By default, the cameras produce a 640x480-pixel color image. For easier image processing, the color image was converted to a (0 - 255) grayscale image. In the examinations, it was seen that the background brightness values varied between 7 and 13 gray brightness values and contained a lot of noise. Therefore, the image was first filtered in a median size of 3x3. Then, a brightness value of 20 was applied to the image as a threshold value to make it easier to find the location of the object in the image. With this operation, all values below 20 are considered as noise and reduced to 0. Pixel values above 20 are left free and considered as objects.

In the next stage, it is necessary to determine the location of the pistachio in the total image in order to get the relevant image instead of the whole image. In order to determine the location of the pistachio, the distribution of all pixels in the image matrix was used. Given the dispersion in the image, it appears that groups of pixels that are non-zero and continue uninterrupted have the potential

to become objects. After determining the starting and ending positions of the object on the matrix, the corresponding region is removed from the main frame (cropped). The crop process makes the processes to be applied from now on work faster. As shown in Figure 39, in images taken from three different cameras of the same pistachio, the area containing the pistachio sample was removed from the main frame.

Figure 39. Matrices covering the pistachio object extracted from the main frame

The features of objects extracted by image processing methods are; total edge length (pistachio perimeter), crack, area, width, length and circularity.

The total edge length (TEL) is the total number of white (255-brightness value) pixels in an image to which the edge detection algorithm has been applied (Figure 40). The Canny - edge detection algorithm was tested to be better than algorithms such as Sobel and Prewitt in calculating the total edge length and it was decided to use it (Ataş 2016a).

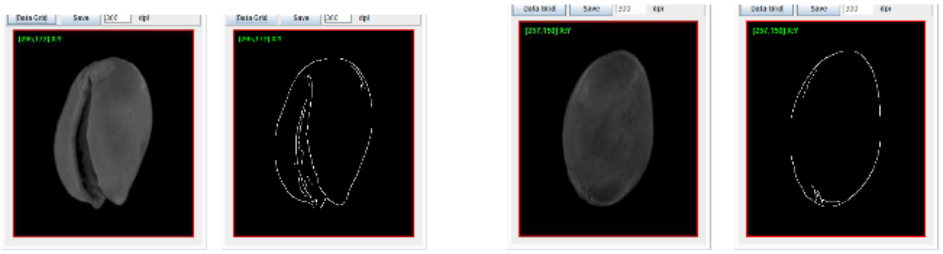

Figure 40. Pistachios with an edge using the Canny edge detection algorithm

The ratio of the total edge length of the pistachio area to the cube root gives information about whether the pistachio is cracked or uncracked. As can be seen from Figure 40 in cracked pistachios, the cracked part is also perceived and taken into account as the edge line. Therefore, the TEL value is increased. Likewise, in pistachios that are not cracked, since only the outer borders of the pistachio have the potential to be edges, the algorithm only calculates the pixels in these nuts

and a low TEL value is obtained. It is often not possible to distinguish between crack and closed pistachios by using only TEL information. Therefore, the TEL value of a small but cracked pistachio may be close to the TEL value of a pistachio that is large but closed. As can be seen in Figure 41, the circumference measurements of two pistachios whose area measurements are close to each other have been quite different due to the crack.

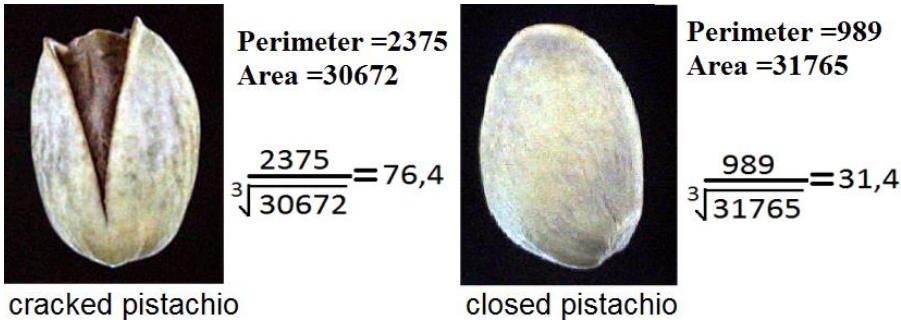

Figure 41. Example pistachio images for the crackedness feature

Due to this special situation, it would be more accurate to use the ratio of the pistachio area of the TEL to the cube root. As a result, it may be possible to detect cracked and closed pistachios regardless of the size of the pistachio. If this feature is called "Edge Area Ratio" (EAR) for short, this value can be obtained with the help of the following equation (Ataş, 2016a).

$$EAR = \frac{TEL}{\sqrt[3]{Area}}$$

The number of pixels to represent the area of the pistachio can be easily done by the previous thresholding. That is, the total number of pixels above 20 pixels is considered the area of the pistachio object.

The pistachio image has two principal axes that are orthogonal to each other. The first axis is the axis of length, which passes longitudinally from the center of the pistachio. The other axis perpendicular to this axis is the width of the pistachio. The algorithm that calculates the length and width tries to find the first, that is, the long axis, in the first place. For this, the brightness value matrix of the cropped pistachio image determines the coordinates of the pixels that are spatially farthest from each other. Then a virtual line is placed between these coordinates. The axis that intersects this virtual line perpendicular is determined. Moving in both directions in the direction of this second axis, the pixels are controlled one by one. Because a threshold value of 20 was previously applied to the image, it moves in the direction of the width in the matrix until it reaches a zero brightness

value. Since the zero gray value will be reached when the pistachios are out, the process is terminated at that point and the total number of pixels is calculated and the width value is determined. Figure 42 shows the state of the basic axes detected for different pistachio samples drawn on the image (Ataş, 2016a).

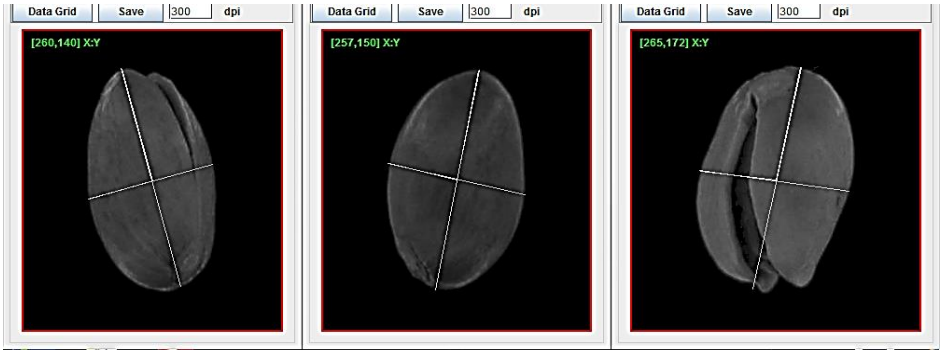

Figure 42. Pistachios with length and width features shown together

Considering the geometry of pistachios, it can be said that the structure is generally similar to an ellipse. For this, a new feature, circularity, is obtained by dividing the Mean length value of each pistachio by the Mean width value of the same pistachio (Figure 43). If the measured value is approaching 1, it indicates that the pistachios are a smooth round. Otherwise, it indicates that it is in the form of an ellipse that is expected to be for pistachios.

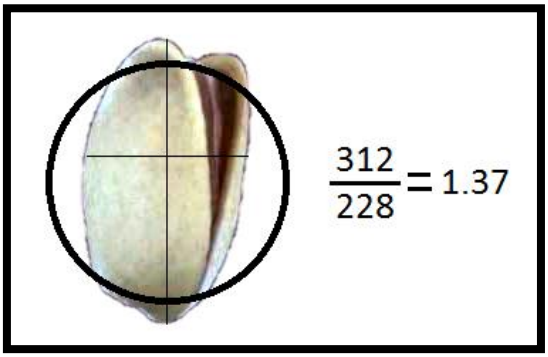

Figure 43. Image of a pistachio with a circularity value of 1,37 units.

Although pistachios are evaluated by weight in the commercial sense, the length, width and therefore the size of each pistachio are also important. For this, estimates of the size of the pistachios were made using pixel measurements obtained from image processing. As is known, cracked large pistachios have more acceptable properties in practice.

For this reason, not only the weight is taken into account in this study, but also the estimation models of the length and width of the pistachio are included. In the regression model for 3 real features to be predicted by pixel measurements; R^2, Adjusted R^2, mean of error squares, AIC (Akaike information criterion), BIC (Bayesian information criterion) and MCp (Mallows' Cp) criteria were taken into account. Of these criteria, the equations used for AIC, BIC and MCp statistics are given below. In determining the best model, it was taken into account that R^2 and Adjusted R^2 were high and the other criteria were low.

$$AIC = n.\ln\left(\frac{\boldsymbol{SSE}}{n}\right) + 2k$$

$$BIC = n.\ln\left(\frac{\boldsymbol{SSE}}{n}\right) + \frac{2(k+2)n\sigma^2}{\boldsymbol{SSE}} - \frac{2n^2\sigma^4}{\boldsymbol{SSE}^2}$$

$$MCp = \frac{\boldsymbol{SSE}}{\sigma^2} + 2k - n$$

However, considering that there may be quadratic and multiplicative relationships in addition to linear relationships, the square of each feature and the binary products of all features were also included in the model as variables. Accordingly, the best model was tried to be determined. SPSS (Ver: 21) statistical package program was used for model calculations.

4. FINDINGS

Descriptive statistics for the features measured in real and virtual in the study are given in Table 1. Correlation coefficients between features are given in Table 2.

Table 1. General descriptive statistics for features

	N	Mean	Standard Deviation	Minimum	Maximum
A_Weight (g)	50	1,117	0,288	0,470	1,640
A_Length (mm)	50	20,170	2,305	13,500	24,000
A_Width (mm)	50	11,507	1,132	9,150	13,750
Perimeter (pixels)	50	1373,355	300,364	816,791	2375,780
Crack (unit)	50	46,890	10,013	31,359	76,430
Area (pixels)	50	26717,190	6589,198	9081,165	38776,090
Width (pixels)	50	155,264	15,815	123,684	196,881
Length (pixels)	50	260,257	33,479	171,266	312,258
Circularity (unit)	50	1,687	0,130	1,328	1,901
$(Perimeter)^2$	50	1974518,812	895994,561	667147,537	5644330,608
$(Crack)^2$	50	2296,930	1033,890	983,390	5841,616
$(Area)^2$	50	756357460	340243600	82467557	15035851556
$(Width)^2$	50	24352,216	4892,707	15297,830	38762,403
$(Length)^2$	50	68832,357	16594,719	29332,282	97505,183
$(Circularity)^2$	50	2,864	0,43192	1,765	3,616
Perimeter x Crack	50	67002,444	29438,929	25613,789	181581,982
Perimeter x Area	50	37403819	13732827	11555401	72870541,862
Perimeter x Width	50	216219,574	63310,536	112892,742	411679,434
Perimeter x Length	50	363220,489	110770,116	149134,281	727775,775
Perimeter x Circularity	50	2324,949	562,886	1107,032	4264,168
Crack x Area	50	1247522,290	387558,996	529424,090	2344295,247
Crack x Width	50	7322,898	1917,499	4321,726	13244,009
Crack x Length	50	12271,166	3325,356	5861,570	23413,045
Crack x Circularity	50	79,211	18,325	42,502	137,181
Area x Width	50	4235560,894	1374479,34	1129136	7634302,518
Area x Length	50	7148652,109	2450461,22	1644109	12108152,066
Area x Circularity	50	45382,426	12471,238	14315,575	67836,255
Width x Length	50	40827,256	8625,800	22204,162	61477,925
Width x Circularity	50	262,079	33,111	172,249	315,873
Length x Circularity	50	441,805	78,985	227,546	560,950

As seen in Table 2, in general, the correlation coefficients between the characteristics were positive and ranged between 0,40 and 0,98. Except for the correlation coefficients between A_Length and cracking, A_Length and $(cracking)^2$, A_Width and circularity and A_Width and $(circularity)^2$, the correlation coefficients between other traits were found to be statistically significant (p<,05). Based on the high correlations thus obtained, regression

equations were written to predict the actual measurement values from the pixel values.

Table 2. Correlation coefficients between variables

	A_Weight (g)	A_Length (mm)	A_Width (mm)
Perimeter (pixels)	0,671**	0,565**	0,705**
Crack (unit)	0,314**	0,214	0,372**
Area (pixels)	0,881**	0,838**	0,806**
Width (pixels)	0,888**	0,720**	0,979**
Length (pixels)	0,942**	0,981**	0,804**
Circularity (unit)	0,415**	0,703**	0,074
$(Perimeter)^2$	0,635**	0,535**	0,666**
$(Crack)^2$	0,304**	0,210	0,354**
$(Area)^2$	0,870**	0,812**	0,792**
$(Width)^2$	0,877**	0,706**	0,972**
$(Length)^2$	0,949**	0,978**	0,807**
$(Circularity)^2$	0,404**	0,694**	0,058
Perimeter x Crack	0,494**	0,395**	0,535**
Perimeter x Area	0,924**	0,829**	0,908**
Perimeter x Width	0,787**	0,648**	0,850**
Perimeter x Length	0,836**	0,770**	0,811**
Perimeter x Circularity	0,712**	0,701**	0,638**
Crack x Area	0,895**	0,797**	0,890**
Crack x Width	0,600**	0,454**	0,689**
Crack x Length	0,681**	0,620**	0,670**
Crack x Circularity	0,411**	0,412**	0,354**
Area x Width	0,902**	0,814**	0,876**
Area x Length	0,919**	0,891**	0,818**
Area x Circularity	0,880**	0,910**	0,719**
Width x Length	0,965**	0,902**	0,929**
Width x Circularity	0,949**	0,980**	0,815**
Length x Circularity	0,825**	0,967**	0,582**

**: p<,05; **: P<,01*

4.1. Weight Estimation

Using the pixel values measured by the machine, three models were created to estimate weight. As independent variables; The Model 1 only included the variables X_1 (Width x Length), the Model 2 had X_1 and X_2 (Width x Circularity), and the Model 3 had X_1, X_2, and X_3 (Circularity). Accordingly, the results of the regression analysis obtained are given in Table 3.

Table 3. Regression analysis results for weight

Model	Variable	Coefficients		R^2	$R^2_{(Adj)}$	MSE	AIC	BIC	MCp
1	X_1	a	-0,200± 0,053	0,931 ± 0,076	0,929	0,005875	-256,88	-254,77	-1,0
		b_1	0,00003226± 0,001						
2	X_1 X_2	a	-0,502± 0,129	0,939 ± 0,072	0,937	0,005167	-261,32	-259,28	3,6
		b_1	0,00002241± 0,001						
		b_2	0,003± 0,001						
3	X_1 X_2 X_3	a	-0,378± 0,126	0,949 ± 0,066	0,946	0,004292	-268,59	-266,77	7,5
		b_1	-0,0000303± 0,001						
		b_2	0,019± 0,005						
		b_3	-1,341± 0,440						

X_1 Width x Length, X_2: Width x Circularity, X_3: Circularity, R^2: Coefficient of Determination, $R^2_{(Adj)}$: Adjusted Determination Coefficient, MSE: Mean Squared Error, AIC: Akaike Information Criteria, BIC: Bayesian Information Criterion, MCp: Mallows' Cp statistic

When Table 3 is examined in terms of regression constants; the constants are negative for all models, with the highest value being obtained from the first model with -0,200. In the regression coefficients, while the coefficients were positive in the first and second models, only the coefficient of X_2 was positive in the third model.

Since the number of explanatory variables added to the model varied between one and three, there was no significant difference between the R^2 and the R^2_{Adj} in all three models and they were found to be close to each other. These values ranged from 92,9% to 94,9% for all three models. Similarly, the AIC and BIC values ranged from -254,77 to -268,59. The Mallows' Cp statistic, which provides information about the relative precision of the model (low variance) is -1 for the first model, while it is 3,6 and 7,5 for the second and third models, respectively.

Accordingly, it is decided that the first model is an appropriate model since the MCp statistic is low and takes a value close to the number of explanatory variables in the model. MSE, AIC and BIC values are lower than the values in

the other models, and R^2 is lower than the other models with a small difference of 1%, but there are fewer independent variables in the model.

Thus, using the pixel values measured by the machine in pistachios, the regression equation proposed to be used to estimate the weight; It can be said that it can be written as follows with a determination coefficient of approximately 93%.

Model 1: Y (Weight) = -0,200 + 0,00003226 X1 (Width x Length)

4.2. Length Estimation

Using the pixel values measured by the machine, three models were created to estimate weight. As independent variable; The Model 1 only included the variables X_1 (Width x Length), the Model 2 had X_1 and X_2 (Width x Circularity), and the Model 3 had X_1, X_2, and X_3 (Circularity). Accordingly, the results of the regression analysis obtained are given in Table 4.

When Table 4 is examined in terms of regression constants; In all three models, the regression constants are positive, with the highest value being obtained from the second model with 4,118. In the regression coefficients, the coefficients of all variables except the X_3 variable in Model 3 were found to be positive.

Table 4. Regression analysis results for length

Model	Variable	Coefficients		R^2	$R^2_{(Adj)}$	MSE	AIC	BIC	MCp
1	X_1	a	2,592± 0,508	0,962 ± 0,4539	0,961	0,2060	-79,03	-76,95	0,005
		b_1	0,068± 0,002						
2	X_1	a	4,118± 0,471	0,978 ± 0,3493	0,977	0,1195	-104,26	-102,02	1,016
		b_1	0,043± 0,004						
	X_2	b_2	0,011± 0,002						
3	X_1	a	2,782± 0,697	0,981 ± 0,3314	0,979	0,1058	-108,60	-106,09	1,94
		b_1	0,053± 0,006						
	X_2	b_2	0,011± 0,002						
	X_3	b_3	-0,000002895± 0,0						

X_1: Length, X_2: Width x Circularity, X_3: Area x Circularity, R^2: Coefficient of Determination, $R^2_{(Adj)}$: Adjusted Determination Coefficient, MSE: Mean Squared Error, AIC: Akaike Information Criteria, BIC: Bayesian Information Criterion, MCp: Mallows' Cp statistic

Since the number of explanatory variables added to the model varied between one and three, no significant difference was observed between the R^2 and the R^2_{Adj} in all three models and they were found to be close values. These values ranged from 92,9% to 94,9% for all three models. Similarly, the AIC and BIC values

ranged from -76,95 to -108,6. MCp statistic, which gives information about the accuracy of the model, was found to be 0,005, 1,016 and 1,94 for the first, second and third models, respectively. Accordingly, it is decided that the first model is an appropriate model since the MCp statistic is low and takes a value close to the number of explanatory variables in the model. The MSE, AIC and BIC values are lower than the values in the other models; and although the coefficient of determination is lower than the other models by a small difference of 2%, there are fewer independent variables in the model.

Thus, it can be said that the regression equation proposed to be used to predict the pistachio length by utilizing the pixel values measured by the machine in pistachios can be written as follows; with a coefficient of determination of approximately 96%.

$$Y\ (\text{Length}) = 2{,}592 + 0{,}068\ X_1\ (\text{Length})$$

4.3. Width Estimation

Using the pixel values measured by the machine, three models were created to estimate width. As independent variables; Model 1 includes only X_1 (Width), Model 2 includes X_1 and X_2 (Cracks x Circularity), Model 3 includes X_1, X_2 and X_3 ((Width)^2) and finally Model 4 includes X_1, X_2, X_3 and X_4 (Area x Circularity). Accordingly, the results of the regression analysis obtained are given in Table 5.

When Table 5 is examined in terms of regression constants; of the four models, the first and second models had positive regression constants; the third and fourth patterns appear to be negative. The highest value for these constant numbers appears to be obtained from the first model with 0,631. When the regression coefficients are examined, it can be seen that the coefficients in all models take positive values.

Table 5. Regression analysis results for width

Model	Variable	Coefficients		R^2	$R^2_{(Adj)}$	MSE	AIC	BIC	MCp
1	X_1	a	0,631± 0,332	0,957 ± 0,2358	0,957	0,055646	-144,48	-142,38	-0,303
		b_1	0,070± 0,002						
2	X_1	a	0,395± 0,289	0,970 ± 0,2015	0,968	0,039771	-159,27	-156,99	0,561
		b_1	0,068± 0,002						
	X_2	b_2	0,007± 0,002						
3	X_1	a	-5,673± 1,933	0,975 ± 0,1845	0,973	0,032646	-167,14	-164,65	2,088
		b_1	0,147± 0,025						
	X_2	b_2	0,007± 0,001						
	X_3	b_3	0,001± 0,001						
4	X_1	a	-7,968± 2,111	0,978 ± 0,1767	0,976	0,029292	-170,56	-167,76	3,355
		b_1	0,173± 0,027						
	X_2	b_2	0,019± 0,006						
	X_3	b_3	0,001± 0,001						
	X_4	b_4	0,001± 0,001						

X_1: Width, X_2: Crack x Circularity, X_3: $(Width)^2$, X_4: Perimeter x Circularity, R^2: Coefficient of Determination, $R^2_{(Adj)}$: Adjusted Determination Coefficient, MSE: Mean Squared Error, AIC: Akaike Information Criteria, BIC: Bayesian Information Criterion, MCp: Mallows' Cp statistic

Since the number of explanatory variables added to the model varied between one and three, no significant difference was observed between the R^2 and the R^2_{Adj} in all three models and they were found to be close values. These values ranged from 92,9% to 94,9% for all three models. Similarly, the AIC and BIC values ranged from -142,38 to -170,56. MCp statistic, which gives information about the accuracy of the model, was found to be 0,561, 2,088 and 3,355 for the first, second, and third models, respectively. Accordingly, it is decided that the first model is an appropriate model since the MCp statistic is low and takes a value close to the number of explanatory variables in the model. The MSE, AIC and BIC values are lower than the values in the other models, and the coefficient of determination is lower than the other models by a small difference of 2%, but there are fewer independent variables in the model.

Thus, the regression equation proposed to be used to predict the width of pistachios using the pixel values measured with the machine; with a coefficient of determination of approximately 96%;

$$Y\ (Width) = 0{,}631 + 0{,}070\ X_1\ (Width)$$ can be written as.

5. DISCUSSION AND CONCLUSION

Today, in parallel with the rapid development of computer technologies, ways are being explored to utilize these technologies as much as possible to facilitate human life. With image processing technologies, significant savings in time and labor can be achieved, although this varies depending on the area where this technology is used. Advances in computer-aided image processing technology have not only improved the quality of the image, but also contributed significantly to the accurate estimation and identification of the features of the imaged objects. The digitalization of images in the computer environment has led to an increase in studies to estimate the real values of the object's features using these numerical values.

Statistical correlation and regression models can be used to determine the relationships between the numeric values that make up the image and the actual properties of the objects. In this context, regression models were created to estimate the actual weight, length and width values of Siirt pistachios by using the pixel values obtained by image processing. In addition to the original variables in the models, new variables were created by taking the multiplicative and quadratic combinations of these variables. Thus, 27 explanatory variables were used to predict the actual values to determine the best model.

In the evaluation of the obtained models; R^2, Adjusted R^2, mean of error squares, AIC, BIC, and MCp criteria were used. Similarly, Elasan and Keskin (2015) stated that AIC and BIC criteria are widely used in determining the best model and emphasized that the model with low values in terms of these values can be preferred.

Considering the criteria for determining the best model, different variables were included in the best prediction model for weight, length and width. In the models agreed for all three features, the determination coefficients were found to be above 93%.

One of the most important quality characteristics of Siirt pistachio is weight. Since weight is directly related to the virtual width, length and circularity of the pistachio obtained by image processing, the best model included the variable "Width x Length", which is the product of width and length. Accordingly, a determination coefficient value of approximately 93% was obtained. Thus, with the variable consisting of the product of the virtual width and length values, it can be said that the actual weight of the pistachios can be estimated correctly by 93%.

For the length and width, which are other quality characteristics of Siirt nuts, respectively; models that include virtual length and virtual width values are best modeled. Thus, it can be said that virtual length values can be used for length and virtual width values can be used for width. If the actual length and width values

are estimated from these values, the degree of accuracy (determination coefficient) in the estimates for both features will be approximately 96%.

Aktan (2004a) aimed to determine the relationships between some egg internal and external quality characteristics and their relationships in Japanese quails by numerical image analysis. For this purpose, regression equations were calculated to predict shell egg area, egg width and length, total egg content, outer watery white, inner dark white and yolk spread areas from digital images of 72 eggs obtained from eight-month-old quail flock. The determination coefficients in the obtained equations ranged from 1% to 92%.

Aktan (2004b) reported that there were statistically significant correlations between some carcass characteristics such as carcass area, breast width, breast length, breast area, breast and abdominal skin color and the values obtained from digital image analysis in 126 broiler chickens slaughtered at 49 days of age.

Zhang et al. (2006) used discrete cosine transform, Laws filters, Gabor filters and matrix-based statistical features in their study. Using a combination of Gabor filter and statistical features, they achieved an 82% success rate in classification.

Acar (2011) investigated the processing of both satellite images and images obtained from medical devices with the same image processing techniques. In this context, he extracted micro-calcification from mammography images and determined buildings from satellite images with the same method. An accuracy rate of approximately 85% was achieved for both studies.

Alaşahan and Günlü (2012) tried to determine the egg quality characteristics of different poultry species by using numerical image analysis in their studies. For this purpose, they used eggs belonging to quail, rock partridge, ringed pheasant and chicken species. As a result, they estimated the height, width and shape values of the eggs by about 98% using image-processing methods.

Ataş (2016a) has made the classification process with the shape-based features of Siirt pistachios using image-processing methods. He used artificial neural networks in the classification and achieved a success rate of 83,33%.

In image, processing, statistical and mathematical methods are used for image color modification, image enhancement, image restoration, edge capture, brightness and contrast adjustment, shape analysis, component analysis, image quality enhancement or reduction, sharpening, rotation, object detection and feature extraction. However, with image processing, the weight and size of the object can be determined using features obtained from the objects in the image.

Image processing analysis, which has been widely used in many areas in recent years, is seen as being available in biological sciences. It is thought that image-processing analysis can provide a significant saving of time and cost in scientific studies. As a result of this study, it can be said that weight, length and

width values, which are important quality characteristics of Siirt pistachio, can be predicted with a high accuracy rate by using pixel values obtained from image processing analysis.

ABSTRACT

Dilbilir Y. The statistical methods used in image processing and an application. Yuzuncu Yil University, Institute of Health Sciences, Department of Biostatistics, Master Thesis, Van 2017. In this study, general information about image processing and statistical methods used in image processing as well as usability of these methods were given and an application was performed. As image processing methods, filtering, image thresholding, image processing, histogram equalization, and mathematical morphology methods were mentioned. Multiple regression equations were found to predict weight, length and width by using virtual measurements obtained from image processing in Siirt pistachio. As well as virtual variables or measurements, new variables are formed by the multiplicative and quadratic combinations of these variables as an explanatory variable in obtaining the regression equations. Thus, 27 explanatory variables were used to find the most appropriate model. Determination coefficient, adjusted determination coefficient, Mean Square Error, Akaike information criterion, Bayesian information criterion and Mallows' Cp criterion were considered to determine the most appropriate model. According to these results; the model consisted of "virtual width x virtual length" was determined as the best model with 93,1% determination coefficient for estimation of weight. Similarly, for length and width, the models formed virtual width and virtual length variables were considered as the best models with 96,2% and 95,7% determination coefficients, respectively. Thus, weight, length and width values that important quality characteristics in Siirt pistachio can be estimated from the virtual pixel values obtained as a result of image processing analysis with highly determination coefficient.

Keywords: Pistachio, pixels, virtual features, multiplicative and quadratic variable, multiple regression

REFERENCES

Acar, U. & Bayram, B. (2009). *Building extraction with morphology*. Paper presented at the Recent Advances in Space Technologies, (pp. 33-38) RAST'09. 4th International Conference on IEEE.

Aktan, S. (2004a). Bıldırcın yumurtalarında bazı iç ve dış kalite özellikleri ile aralarındaki ilişkilerin sayısal görüntü analizi ile belirlenmesi. *Hay Üret, 45* (1), 7-13.

Aktan, S. (2004b). Sayısal görüntü analizi ile etlik piliçlerde bazı karkas özelliklerinin belirlenmesi. *Hayvansal Üretim,* 45(1), 14-18.

Alaşahan, S. Günlü, A. (2015). Farklı kanatlı türlerinde yumurta kalite özelliklerinin sayısal görüntü analizi ile belirlenmesi. *Kafkas Üniversitesi Veteriner Fakültesi Dergisi,* 18(6) 979-986.

Anonymous (2003). https://tekrei.gitlab.io/other/2003-Goruntu-Isleme.pdf. Access date: 09.10.2023

Anonymous (2016). https://www.miniphysics.com/electromagnetic-spectrum_25.html Access date: 09.10.2023

Anonymous (2019). https://rpg.ifi.uzh.ch/docs/teaching/2019/04_filtering.pdf. Access date: 09.10.2023

Arslan, E. (2011). *Hücresel Sinir Ağı Sistemleri Kullanarak Hareketli Nesnelerin Görüntü İşleme Uygulamaları*. İstanbul Üniversitesi, Fen Bilimleri Enstitüsü, Yüksek Lisan Tezi, İstanbul.

Aslantaş, A. (2006). *Bir Ağaç Kesitindeki Yıllık Halkaların Görüntü İşleme Yöntemi ile İncelenmesi*. Süleyman Demirel Üniversitesi, Fen Bilimleri Enstitüsü, Yüksek Lisans Tezi, Isparta.

Asmaz, K. (2006). *Görüntü İşleme ile İki Boyutlu Cisimlerden Grafik Modeller İçin Veri Eldesi*. Yıldız Teknik Üniversitesi, Fen Bilimleri Enstitüsü, Yüksek Lisans Tezi, İstanbul.

Ataş M. (2016b). Open Cezeri Library: A novel java-based matrix and computer vision framework. *Comp Appl Eng Educ*, 24(5), 736-743.

Ataş, M. (2016a). Fıstık sınıflandırma sistemi için Siirt fıstığı imgelerinden gürbüz özniteliklerin çıkarılması. *DÜMF Mühendislik Dergisi*, 7(1), 93-102.

Bal, H. (2006). *Kamera ile Görüntü İşleme Teknikleriyle Malzeme Tane Büyüklüğü Analizi.* Gazi Üniversitesi, Fen Bilimleri Enstitüsü, Yüksek Lisan Tezi, Ankara.

Bellanger, M. (2000). Reviews and New Releases: Digital Signal Processing of Signals. Theory and Practice. *Trans Emerging Tel Technology, 11*(6) 617-618.

Bennamoun, M. & Boashash, B. (1997). A structural-description-based vision system for automatic object recognition. *IEEE Trans Syst Man Cybern, Part B (Cybernetics)*, 27(6), 893-906.

Bozkurt, K. (2009). *Retina Görüntülerinin Ayrıştırılması*. Düzce Üniversitesi, Fen Bilimleri Enstitüsü, Yüksek Lisan Tezi, Düzce.

Bushberg, J. T.; Seibert, J. A.; Leidholdt, Jr EM; Boone, J. M. (2011). The Essential Physics of Medical Imaging. *Lippincott Williams and Wilkins*. Philadelphia, USA.

Çankaya, G. (2013). *Görüntü İşleme Teknolojisi ile Betonun Bazı Mekanik Özelliklerinin Belirlenmesi.* Selçuk Üniversitesi, Fen Bilimleri Enstitüsü, Yüksek Lisan Tezi, Konya.

Çavdaroğlu, G. Ç. (2013). Smart facial feature regions and facial feature points. *J Eng Nat Sci*, Sigma, (31), 246-261.

Çelik, E. (2014). *Görüntü İşlemeye Dayalı Avuç İçi İzinin Yapay Sinir Ağı ile Tanınması.* Marmara Üniversitesi, Fen Bilimleri Enstitüsü, Yüksek Lisans Tezi, İstanbul.

Crane, R. (1996). Simplified approach to image processing, classical and modern techniques in C. Prentice Hall PTR, Upper Saddle River, NJ, USA.

Ding L, Goshtasby & A, Satter M. (2001). Volume image registration by template matching. Ima Vis Comp, 19(12) 821-832.

Doğan, Y. & Ataş, M. (2015). *Prediction of adaptive exposure time in hyperspectral bands for industrial cameras.* Paper presented at the Signal Processing and Communications Applications Conference (SIU), 16.05.2015, 23th, Malatya.

Doğan, Y. & Ataş, M. (2016) *Classification of Siirt and Gaziantep Pistachio nuts based on Computer Vision*, İnternational conference on artificial intelligence and data processing, 17.09.2016, (IDAP16), Malatya.

Doğan, Y. (2016). *Endüstriyel Kameralar İçin Hiperspektral Bantlarda Adaptif Pozlama Süresi Kestirimi*. Fırat Üniversitesi, Fen Bilimleri Enstitüsü, Yüksek Lisans Tezi, Elâzığ.

Duda, RO; Hart, PE; & Stork, DG. (2001). Pattern classification. *Int J Comput Intell Appl*, (1), 335-339.

Edizer, E. (2006). *Sayısal Görüntü İşleme Yöntemi ile Tane Boyut Dağılımı Analizi.* Çukurova Üniversitesi, Fen Bilimleri Enstitüsü, Yüksek Lisans Tezi, Adana.

Elasan, S. & Keskin, S. (2015). An application with multinomial logistic regression analysis. *Int J Hum Sci*, 12(1), 43-45.

Fu, LC & Liu, CY (2001). *Computer vision-based object detection and recognition for vehicle driving*. Paper presented at the Robotics and Automation, Proceedings ICRA. IEEE International Conference, Korea.

Ghazanfari, A; Irudayaraj, J; Kusalik, A & Romaniuk, M. (1997). Machine vision grading of pistachio nuts using Fourier descriptors. J Agr Eng Res (68)3, 247-252.

Ghezelbash, J; Borghaee, AM & Minaei, SM. (2011). Automated sorting of closed-shell pistachio nuts using machine vision system. *World Appl Sci J 12*(11), 1989-1995.

Göktaş, D. (2012). *Video Görüntüleri İçinden Hareketli Nesne Ayıklanması ve İzlenmesi*. Fırat Üniversitesi, Fen Bilimleri Enstitüsü, Yüksek Lisans Tezi, Elâzığ.

Gonzalez, R. C. (2009). Digital image processing. Pearson education, India.

Gonzalez, R. C.; Eddins, SL & Woods, RE. (2004). *Digital Image Processing Using MATLAB. Prentice Hall Press,* Upper Saddle River, Nev Jersey, USA

Johnson S (2006). *Stephen Johnson on digital photography*. O'Reilly Media, Inc, USA.

Karakoç, M. (2011). *Görüntü İşleme Teknikleri ve Yapay Zekâ Yöntemleri Kullanarak Görüntü İçinde Görüntü Arama*. Pamukkale Üniversitesi, Fen Bilimleri Enstitüsü, Yüksek Lisans Tezi, Pamukkale.

Marchand-Maillet, S. & Sharaiha, YM, (1999). *Binary digital image processing: a discrete approach*. Academic Press, London.

McAndrew, A. (2004). *An introduction to digital image processing with matlab notes for scm2511 image processing*. School of Computer Science and Mathematics, Victoria University of Technology, Australia.

Metlek, S. (2009). *Üretim Bandı Üzerindeki Renkli Silindir Parçalarının Makine Görme Sistemiyle Tanımlanması ve Sınıflandırılması*. Süleyman Demirel Üniversitesi, Fen Bilimleri Enstitüsü, Yüksek Lisans Tezi, Isparta.

Mutlu, G. (2011). *Görüntü İşleme Tabanlı Konum Denetimi*. Gazi Üniversitesi, Fen Bilimleri Enstitüsü, Yüksek Lisan Tezi, Ankara.

Ok, A; Wegner, J; Heipke, C; Rottensteiner, F; Sörgel, U & Toprak, V. (2010). *Çok Bantlı Stereo Hava Fotoğraflarından Doğrusal Çizgilerin Otomatik Geri-Çatımı İçin Yeni Bir Yaklaşım*. III. Uzaktan Algılama ve Coğrafi Bilgi Sistemleri Sempozyumu, 11.10.2010, Kocaeli.

Okur, S. (2015). *Görüntü İşleme Yöntemleri Kullanılarak Gözdeki Damarların Tespit Edilmesi.* Fırat Üniversitesi, Fen Bilimleri Enstitüsü, Yüksek Lisans Tezi, Elâzığ.

Omid, Mahmoud. (2011). Design of an expert system for sorting pistachio nuts through decision tree and fuzzy logic classifier. Expert Syst Appl (38)4, 4339-4347.

Özdemir, K. (2004). *Dijital Görüntü İşleme Tekniği ile Patlatma Verimlilik Analizi.* İstanbul Üniversitesi, Fen Bilimleri Enstitüsü, Yüksek Lisans Tezi, İstanbul.

Perihanoğlu, GM. (2015). *Dijital Görüntü İşleme Teknikleri Kullanılarak Görüntülerden Detay Çıkarımı*. İstanbul Teknik Üniversitesi, Fen Bilimleri Enstitüsü, Yüksek Lisans Tezi, İstanbul.

Pitas, I. (2000). *Digital image processing algorithms and applications*. John Wiley and Sons, New York.

Qidwai, U. & Chen, CH. (2009). *Digital image processing: an algorithmic approach with Matlab.* CRC press, USA.

Russ, JC. & Brent Neal, F. (2016). *The image-processing handbook*. Seventh edition, CRC press, USA.

Russ, JC. & Woods, RP. (1995). The *image processing handbook*. CRC press, USA.

Serra, J. (1982). *Image analysis and mathematical morphology V1*. Academic press, London

Sharma, B., & Dadwal, J. (2015). Design of image processing technique in digital enhancement application. *International Journal of Advances in Scientific Research, 1*(8), 340-342.

Sinha, SK. Fieguth, PW. (2006). Morphological segmentation and classification of underground pipe images. Mach Vision Appl (17)1, 21-31.

Ünal, Y; Aktürk, N. & Eroğlu, M. (1999). Seri üretim hatlarında görüntü işlemeyle kalite kontrolü. *Gazi Üniv Fen Bilimleri Enstitüsü Dergisi, (12)*4.

Yakut, H. (2013). *İşaret Dili Harflerinin Görüntü İşleme Yöntemleriyle Tanınması İçin Bir Uygulama*. Fırat Üniversitesi, Fen Bilimleri Enstitüsü, Yüksek Lisan Tezi, Elâzığ.

Young, IT; Gerbrands, JJ & Van Vliet, LJ. (1998). *Fundamentals of image processing.* Delft University of Technology, Delft.

Zhang, X; Krewet, C. & Kuhlenkötter, B. (2006). Automatic classification of defects on the product surface in grinding and polishing. *Int J Mach Tools Manuf (46)*1, 59-69.